(a)

RT-PCR

chronic exposure

(b)   (c)

N=4
(mg/ml)

Fig. 3 Intracellular content of aluminum. Cells underwent short- or long-term incubation with Al-maltol. The treated cells were harvested and freeze-dried, followed by measurement of the intracellular aluminum content by atomic absorbance spectrometry. The data were obtained from four separate experiments (mean ± SE).

Fig. 2 Effect of chronic incubation with low concentrations of Al-maltol on hypoxia-induced expression of PS2V in SK-N-SH cells. SK-N-SH cells were cultured for three months in α-MEM (10% FCS) containing 2.5 or 25 μM Al-maltol, followed by hypoxic stimulation. Cells were harvested at 0–8 h after hypoxia and total RNA was prepared for RT-PCR of PS2V. (a) Representative data was shown (2.5 μM). RT-PCR-amplified products were separated on a polyacrylamide gel and visualized by ethidium bromide staining. Arrows indicate the positions of the normal PS2 transcript and the aberrant PS2V transcript. (b and c) Quantitative data were obtained by densitometry of the band corresponding to the molecular weight of PS2V (shown as a percentage of control).

(a) **western blotting**

(b) **UV-cross link**

Fig. 4 Effect of Al-maltol on hypoxia-induced HMGA1a expression in SK-N-SH cells. SK-N-SH cells were incubated with Al-maltol for 6 h or 3 months. The treated cells were then exposed to hypoxia for 6 h, followed by preparation of either nuclear fractions (a) or nuclear extracts (b). (a) Nuclear fractions were subjected to SDS–PAGE (15%) after immunoblotting using an anti-HMGA1a antibody. The arrow indicates the position of HMGA1a protein (~18 kDa). (b) Nuclear extracts were analyzed by the UV cross-linking assay with no. 5 probe and subjected to SDS–PAGE (15% gel). The no. 5 probe is an RNA probe that has the sequence which HMGA1a specifically recognizes (Manabe *et al.* 2003). The arrow indicates the position of HMGA1a protein.
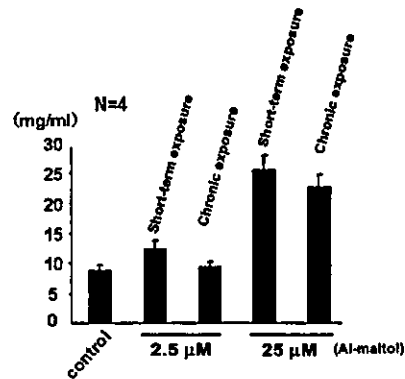
concentration dependence of the induction of PS2V expression was not observed.

Intracellular aluminum content of SK-N-SH cells exposed to Al-maltol for 3 months

Next we investigated the accumulation of aluminum after short-term and chronic exposure of SK-N-SH cells to a low concentration Al-maltol by using the atomic absorbance spectrometry. As a result, intracellular accumulation of aluminum increased in an Al-maltol concentration-dependent manner after both brief and chronic exposure (Fig. 3). However, aluminum accumulation was not dependent on the duration of exposure in this experiment. Therefore, our findings raised the possibility that the acceleration by chronic low concentration of aluminum depends on the incubation period, but is not related to intracellular accumulation of aluminum during chronic exposure of SK-N-SH cells.
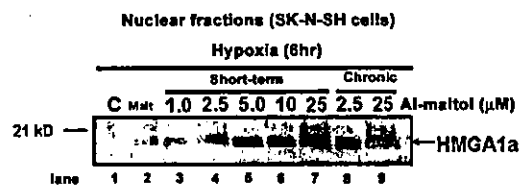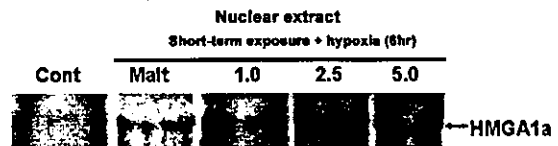
Induction of HMGA1a by Al-maltol incubation

It had been demonstrated that PS2V is generated by HMGA1a in SK-N-SH cells (Manabe *et al.* 2003). Consequently, we investigated the effect of Al-maltol on expression of hypoxia-induced HMGA1a in SK-N-SH cells. Significant expression of HMGA1a protein was not observed in SK-N-SH cells after hypoxic stimulation for 6 h (Fig. 4a, lane 1).

However, expression of HMGA1a protein was increased in Al-maltol-treated cells (short-term exposure) after 6 h of hypoxia, compared with control cells and the increase was dependent on the Al-maltol concentration (Fig. 4a, lanes 2–7).

At this time, the binding of HMGA1a to its recognition RNA sequence (no. 5 RNA probe; length 41nt) was significantly increased in a dose-dependent manner (Fig. 4b).

Strong HMGA1a immunoreactivity was observed in nuclear fractions isolated from chronic exposed Al-maltol-treated SK-N-SH cells after 6 h of hypoxia (Fig. 4a, lanes 8 and 9).

Aluminum promotes cell death by endoplasmic reticulum (ER) stress

We previously demonstrated that cells expressing PS2V or exposed to hypoxia exhibited increased vulnerability to various ER stresses, the mechanism of which was related to the down-regulation of UPR signaling (Sato *et al.* 2001; Manabe *et al.* 2003). To confirm that the increase of PS2V production induced by Al-maltol under hypoxic conditions reflected an increase in susceptibility to ER stress, we investigated cell death on the basis of morphological changes (Fig. 5). Cell death induced by tunicamycin (Tm), which is a major ER stress inducer, was significantly promoted by hypoxia, consistent with previous observations (Manabe *et al.* 2003). This promotion was accelerated by chronic exposure to Al-maltol at a concentration of 2.5 μM (Fig. 5b) or 25 μM (data not shown). From 6 to 12 h after Tm treatment, the extent of cell death was different between Al-maltol-treated and untreated (control) cultures. On the other hand, under the normoxic condition, the extent of cell death was unaffected by short-term incubation with Al-maltol at a concentration of 25 or 1000 μM, nor by chronic exposure to 2.5 or 25 μM (Fig. 5a). Consequently, it was clarified that cells exposed to Al-maltol were more sensitive to ER stress, · as was observed for cells expressing PS2V. Finally, we compared chronic Al-maltol treated group with control group on the ratio of extent of cell death by Tm plus hypoxia treatment to the extent by Tm alone treatment (Fig. 5c). In every indicated time, the ratio by Tm + Hypo was higher than the ratio by Tm alone. This result suggested that effect of chronic Al-maltol exposure is acceleration to hypoxia (means production of PS2V) but not enhancement to Tm toxicity.

Discussion

We examined the effects of transient exposure to various metal salts ($FeCl_2$, $FeCl_3$, $CuCl_2$, $CuSO_4$, $ZnCl_2$, $AlCl_3$, and Al-maltol). However, except in the case of aluminum, the same level of PS2V production was not detected between experiments using the same concentration of each metal. In contrast, addition of $AlCl_3$ and Al-maltol reproducibly caused the production of PS2V. Abnormalities of iron, copper and zinc have been reported as risk factors for the onset of AD. However, it is difficult to monitor the intracellular content of these metals and distinguish endogenous from exogenous sources because each of these metals is required by living cells. On the contrary, aluminum is not a necessary metal for cells, so it is relatively easy to estimate the effect of aluminum treatment by measuring its content in the target cells. In the present study, we therefore focused on the influence of aluminum as a proxy for various metals.
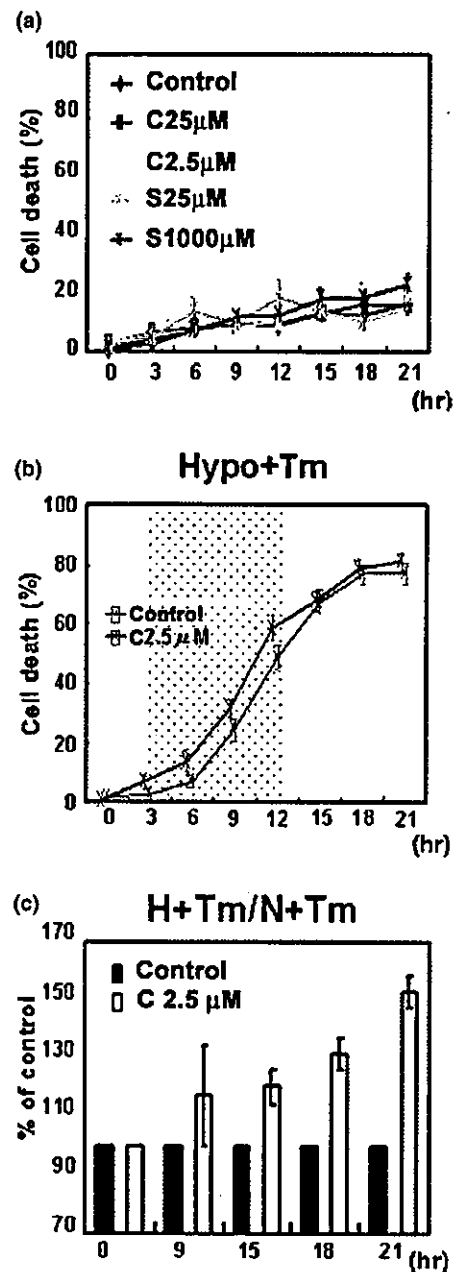
Fig. 5 Effect of Al-maltol on cell death associated with PS2V expression in SK-N-SH cells exposed to ER stress. (a) Viability of SK-N-SH cells with chronic (C) or short-termed (S) Al-maltol-treatment under normoxia for 21 h, followed by assay of morphological changes. (b) The effects of Al-maltol treatment on SK-N-SH cell viability under hypoxia exposure plus tunicamycin (Tm) stress (ER stress) were evaluated by counting of morphological changes in indicated time. The cells were treated with 0.5 μg/mL Tm and exposed to hypoxia. Data are shown as a percentage of the control value (0 h) (mean ± SE). (c) Comparison between chronic Al-maltol treated group (C2.5) and control group (control) on the ratio (cell death score by Tm treatment plus hypoxia exposure to the score by Tm treatment alone: Hypoxia + Tm/Normoxia + Tm). Data are shown as a percentage of the control group ratio.

Production of PS2V was slightly induced by 25 or 250 μM Al-maltol without hypoxia. Under hypoxic conditions, however, PS2V was more strongly and rapidly expressed after exposure to Al-maltol treatment. At 24 h after hypoxia, it was interesting that 250 μM Al-maltol induced less PS2V than 25 μM. This suggested that excessive oxidative stress did not induce production of PS2V, consistent with our previous report that exposure to H_2O_2 did not induce PS2V (Sato *et al.* 1999).

Chronic Al exposure accelerates PS2V production

Exposure to a low (2.5 μM) or moderate (25 μM) concentration of Al for 3 months caused an increase in the production of PS2V after hypoxic exposure, but there was no difference in the increment of PS2V production between both concentrations (Fig. 3). To determine whether the increment of PS2V production was based on the accumulation of aluminum or chronic stimulation, we measured the intracellular content of aluminum by atomic absorbance spectrometry. Interestingly, there was no further increase of intracellular aluminum in SK-N-SH cells by long-term exposure to Al-maltol despite an increase of the cellular aluminum content according to the concentration of Al-maltol. This finding suggests that the acceleration of PS2V production was caused by chronic aluminum exposure, but did not depend on the aluminum concentration.

HMGA1a expression is induced by Al-maltol

Recently, we reported that HMGA1a is a mediator of aberrant PS2 pre-mRNA splicing and the production of a deleterious PS2V protein (Manabe *et al.* 2003). In that experiment, HMGA1a was inducible by hypoxia only in a neuronal cell line. In the present study, HMGA1a was dose-dependently induced by Al-maltol (Fig. 4a). The induction of HMGA1a was increased by long-term exposure of SK-N-SH cells to Al-maltol, and the nuclear extract containing HMGA1a bound to a specific sequence on PS2 pre-mRNA exon 5, which was located upstream of the 5′ splicing site (Fig. 4b). These results indicate that production of PS2V stimulated by Al-maltol occurred by an equivalent mechanism to production due to hypoxia.

Neuronal cell death and aluminum

Chronic aluminum neurotoxicity is well known on the basis of the fact that dialysis dementia occurs in adults and children with renal insufficiency who are treated with aluminum-contaminated dialysate solutions or oral phosphate-binding agents that contain aluminum (Alfrey *et al.* 1976; American Academy of Pediatrics Committee on Nutrition 1986). However, most previous studies about the relationship between aluminum and AD have assessed the effects of high doses of aluminum. For example, transient or chronic administration of 60–8300 mg/kg p.o., 1–60 mg i.v., or 0.1–5 mg i.c.v. *in vivo* and 100–1000 μM *in vitro* were tested in the previous studies (Gawlick *et al.* 1987; Martyn

et al. 1989; ATSDR 1999). On the contrary, we used low concentrations of 2.5–25 μM *in vitro*, and these levels are known not to show neurotoxicity (Alfrey *et al.* 1976). Consequently, there are differences between high-dose aluminum toxicity in dialysis dementia and the effect of low concentrations of aluminum shown in the present study. In spite of the low concentration, cell death induced by ER stress and/or by hypoxia was promoted by chronic exposure to aluminum. The reasons are unclear, but it is thought that oxidative stress was at least partly involved in this promotion of cell death. Although aluminum salts do not stimulate peroxidation per se, these salts greatly accelerate peroxidation induced by iron(II) salts (Savory *et al.* 1999). Also, our previous study showed that pretreatment of SK-N-SH cells with antioxidants before exposure to hypoxia could completely suppress the production of PS2V (Sato *et al.* 1999). Taken together, our data suggest that the combined stresses of hypoxia and ROS generation by metals including aluminum are necessary to trigger an increase of PS2V and consequent vulnerability to ER stress.

In conclusion, our findings suggest that some metals at low concentrations can accelerate and enhance PS2V generation. Accordingly, exposure to hypoxia plus the long-term intake of such metals at low concentrations may promote the development of AD. Consequently, such hypothesis may provide to shed light on the pathogenesis and development of sporadic cases of AD.

References

Alfrey A. C., LeGendre G. R. and Kaehny W. D. (1976) The dialysis encephalopathy syndrome: possible aluminum intoxication. *N. Engl. J. Med.* 294, 184–188.

American Academy of Pediatrics Committee on Nutrition (1986) Aluminum toxicity in infants and children. *Pediatrics* 78, 1150–1154.

ATSDR (1999) *Toxicological Profile for Aluminum (Update): Agency for Toxic Substances and Disease Registry (ATSDR)*. U.S. Department of Health and Human Services, USA.

Borgem D. R. and Essig D. A. (1998) Induction of HSP 32 gene in hypoxic cardiomyocytes is attenuated by treatment with N-acetyl-L-cystein. *Am. J Physiol.* 274, H965–H973.

Bush A. I. (2003) The metallobiology of Alzheimer's disease. *Trends Neurosci.* 26, 207–214.

Crapper D. R., Quittkat S., Krishnan S. S., Dalton A. J. and DeBoni U. (1980) Intranuclear aluminum content in Alzheimer's disease, dialysis encephalopathy, and experimental aluminum encephalopathy. *Acta Neuropathol. (Berl.)* 50, 19–24.

Curtain C. C., Ali F., Volitakis I., Cherny R. A., Norton R. S., Beyreuther K., Barrow C. J., Masters C. L., Bush A. I. and Barnham K. J. (2001) Alzheimer's disease amyloid-beta binds copper and zinc to

generate an allosterically ordered membrane-penetrating structure containing superoxide dismutase-like subunits. *J. Biol. Chem.* **276**, 20466–20473.

Finnegan M. M., Retting S. J. and Orvig C. (1986) A neutral water-soluble aluminum complex of neurological interest. *J. Am. Chem. Soc.* **108**, 5033–5035.

Gawlick D., Bratter P., Gatschke W. and Meyer-Sabellek W. (1987) Aluminum in the Maintenance Diet of Rats, In: *Trace Element Analytical Chemistry in Medicine and Biology* (P. Bratter and P. Schramel, eds), Vol. 4, pp. 431–442. Walter de Gruyter Co., New York.

Goate A., Chartier-Harlin M. C., Mullan M. *et al.* (1991) Segregation of a missense mutation in the amyloid precursor protein gene with familial Alzheimer's disease. *Nature* **349**, 704–706.

Katayama T., Imaizumi K., Sato N. *et al.* (1999) Presenilin-1 mutations downregulate the signalling pathway of the unfolded-protein response. *Nat. Cell. Biol.* **1**, 475–485.

Kennard M. L., Feldman H., Yamada T. and Jefferies W. A. (1996) Serum levels of the iron binding protein p97 are elevated in Alzheimer's disease. *Nat. Med.* **2**, 1230–1235.

Linder M. C. and Hazegh-Azam M. (1996) Copper biochemistry and molecular biology. *Am. J. Clin. Nutr.* **63**, 797S–811S.

Loeffler D. A., Connor J. R., Juneau P. L., Snyder B. S., Kanaley L., DeMaggio A. J., Nguyen H., Brickman C. M. and LeWitt P. A. (1995) Transferrin and iron in normal, Alzheimer's disease, and Parkinson's disease brain regions. *J. Neurochem.* **65**, 710–716.

Manabe T., Kitayama T., Ogita K. and Yoneda Y. (2000) Differential expression and phosphorylation of particular Fos family members by kainate in nuclear and cytosolic fractions of murine hippocampus. *Neuroscience* **100**, 453–463.

Manabe T., Kuramoto N., Nakamichi N., Aramachi K., Baba K., Hirai T., Yoneyama M. and Yoneda Y. (2001a) Degradation of c-Fos protein expressed by N-methyl-D-aspartic acid in nuclear fractions of murine hippocampus. *Brain Res.* **905**, 34–43.

Manabe T., Ogita K., Nakamichi N. and Yoneda Y. (2001b) Differential *in vitro* degradation of particular Fos family members expressed by kainic acid in nuclear and cytosolic fractions of murine hippocampus. *J. Neurosci. Res.* **64**, 34–42.

Manabe T., Katayama T., Sato N., Kudo T., Matsuzaki M., Imaizumi K. and Tohyama M. (2002) The cytosolic inclusion bodies that consists of splice variants that lack exon 5 of the presenilin-2 gene differ obviously from Hirano bodies observed in the brain from sporadic cases of Alzheimer's disease patients. *Neurosci. Let.* **328**, 198–200.

Manabe T., Katayama T., Sato N. *et al.* (2003) Induced HMGA1a expression causes aberrant splicing of presenilin-2 pre-mRNA in sporadic Alzheimer's disease. *Cell Death Differ.* **10**, 698–708.

Markesbery W. R. (1997) Oxidative stress hypothesis in Alzheimer's disease. *Free Radic. Biol. Med.* **23**, 134–147.

Martyn C. N., Barker D. J., Osmond C., Harris E. C., Edwardson J. A. and Lacey R. F. (1989) Geographical relation between Alzheimer's disease and aluminum in drinking water. *Lancet* **14**, 1 (8629), 59–62.

Meshitsuka S. and Inoue M. (1998) Urinary excretion of aluminum from antacid ingestion and estimation of its apparent biological half-time. *Trace Elements Electroly.* **15**, 132–135.

Meshitsuka S., Matsushima F. and Nose T. (1999) Absorption of aluminum from aspirin preparations with aluminum glycinate. *Trace Elements Electroly.* **16**, 175–176.

Multhaup G. (1997) Amyloid precursor protein, copper and Alzheimer's disease. *Biomed. Pharmacother.* **51**, 105–111.

Multhaup G., Schlicksupp A., Hesse L. *et al.* (1996) The amyloid precursor protein of Alzheimer's disease in the reduction of copper (II) to copper (I). *Science* **271**, 1406–1409.

Multhaup G., Masters C. L. and Beyreuther K. (1998) Oxidative stress in Alzheimer's disease. *Alzheimer Rep.* **1**, 147–154.

Pratico D., Uryu K., Sung S., Tang S., Trojanowski J. Q. and Lee V. M. (2002) Aluminum modulates brain amyloidosis through oxidative stress in APP transgenic mice. *FASEB J.* **16**, 1138–1140.

Rogaev E. I., Sherrington R., Rogaeva E. A. *et al.* (1995) Familial Alzheimer's disease in kindreds with missense mutations in a gene on chromosome 1 related to the Alzheimer's disease type 3 gene. *Nature* **376**, 775–778.

Sato N., Hori O., Yamaguchi A. *et al.* (1999) A novel presenilin-2 splice variant in human Alzheimer's disease brain tissue. *J. Neurochem.* **72**, 2498–2505.

Sato N., Imaizumi K., Manabe T. *et al.* (2001) Increased production of β-amyloid and vulnerability to endoplasmic reticulum stress by an aberrant spliced form of presenilin-2. *J. Biol. Chem.* **276**, 2108–2114.

Savory J., Rao J. K., Huang Y., Letada P. R. and Herman M. M. (1999) Age-related hippocampal changes in Bcl-2. Bax ratio, oxidative stress, redox-active iron and apoptosis associated with aluminum-induced neurodegeneration: increased susceptibility with aging. *Neurotoxicology.* **20**, 805–817.

Schreiber E., Matthias P., Muller M. M. and Schaffner W. (1989) Rapid detection of octamer binding proteins with 'mini-extracts', prepared from a small number of cells. *Nucleic Acids Res.* **17**, 6419.

Selkoe D. J. (1994) Normal and abnormal biology of the beta-amyloid precursor protein. *Annu. Rev. Neurosci.* **17**, 489–517.

Smith M. A., Richey Harris P. L., Sayre L. and Perry G. (1997) Iron accumulation in Alzheimer disease is a source of redox-generated free radicals. *Proc. Natl Acad. Sci. USA* **94**, 9866–9868.

White A. R., Huang X., Jobling M. F., Barrow C. J., Beyreuther K., Masters C. L., Bush A. I. and Cappai R. (2001) Homocysteine potentiates copper- and amyloid beta peptide-mediated toxicity in primary neuronal cultures: possible risk factors in the Alzheimer's-type neurodegenerative pathways. *J. Neurochem.* **76**, 1509–1520.

Yoneda Y., Ogita K., Azuma Y., Ikeda M., Tagami H. and Manabe T. (1999) N-Methyl-D-aspartate signaling to nuclear activator protein-1 through mechanisms different from those for kainate signaling in murine brain. *Neuroscience* **90**, 519–533.

Article

Involvement of caspase-4 in endoplasmic reticulum stress-induced apoptosis and Aβ-induced cell death

Junichi Hitomi,[1,6] Taiichi Katayama,[1,6] Yutaka Eguchi,[2,6,7] Takashi Kudo,[3] Manabu Taniguchi,[1,6]
Yoshihisa Koyama,[1,6] Takayuki Manabe,[1,6] Satoru Yamagishi,[1,6] Yoshio Bando,[4] Kazunori Imaizumi,[5]
Yoshihide Tsujimoto,[2,6,7] and Masaya Tohyama[1,6]

[1]Department of Anatomy and Neuroscience, [2]Division of Molecular Genetics, and [3]Division of Psychiatry and Behavioural
  Proteomics, Department of Post-Genomics and Diseases, Graduate School of Medicine, Osaka University, Suita,
  Osaka 565-0871, Japan
[4]Department of Anatomy, Asahikawa Medical College, Midorigaoka Higashi, Asahikawa, Hokkaido, 078-8510, Japan
[5]Division of Structural Cell Biology, Nara Institute of Science and Technology, Takayama, Ikoma, Nara 630-0101, Japan
[6]21st Century COE Program, Japan Society for the Promotion of Science, Chiyoda-ku, Tokyo 102-8471, Japan
[7]Solution Oriented Research for Science and Technology of Japan, Science and Technology Agency, Honcho 4-1-8, Kawaguchi,
  Saitama, 332-0012, Japan

Recent studies have suggested that neuronal death in Alzheimer's disease or ischemia could arise from dysfunction of the endoplasmic reticulum (ER). Although caspase-12 has been implicated in ER stress-induced apoptosis and amyloid-β (Aβ)–induced apoptosis in rodents, it is controversial whether similar mechanisms operate in humans. We found that human caspase-4, a member of caspase-1 subfamily that includes caspase-12, is localized to the ER membrane, and is cleaved when cells are treated with ER stress-inducing reagents, but not with other apoptotic reagents. Cleavage of caspase-4 is not affected by overexpression of Bcl-2, which prevents signal transduction on the mitochondria, suggesting that caspase-4 is primarily activated in ER stress-induced apoptosis. Furthermore, a reduction of caspase-4 expression by small interfering RNA decreases ER stress-induced apoptosis in some cell lines, but not other ER stress-independent apoptosis. Caspase-4 is also cleaved by administration of Aβ, and Aβ-induced apoptosis is reduced by small interfering RNAs to caspase-4. Thus, caspase-4 can function as an ER stress-specific caspase in humans, and may be involved in pathogenesis of Alzheimer's disease.

Introduction

Recently, it has been reported that some human diseases, such as Alzheimer's disease (AD), Parkinson's diseases, and cystic fibrosis, and neuronal damage by ischemia are related to stress acting on the ER, which leads to intraluminal accumulation of unfolded proteins (Katayama et al., 1999; Wigley et al., 1999; Imai et al., 2000, 2001; Nakagawa et al., 2000; Sato et al., 2001; Tamatani et al., 2001). Stress on the ER can be induced in vitro by depletion of calcium from the ER lumen, inhibition of asparagine N-linked glycosylation,

reduction of disulfide bonds, expression of mutant proteins, and ischemia (Imaizumi et al., 2001). ER stress induces three major cellular responses: unfolded protein response (UPR), ER-associated degradation, and apoptosis. Cells exposed to ER stress can up-regulate genes encoding chaperones that facilitate the protein folding process in the ER and reduce overall translation (UPR; Harding et al., 1999; Kaufman, 2002; Forman et al., 2003), or enhance proteasomal degradation of misfolded ER protein in cytosol (Bonifacino and Weissman, 1998; Travers et al., 2000), to reduce the accumulation and aggregation of misfolded proteins, and relieve cells from the stress (Kozutsumi et al., 1988). On the other hand, excessive or long-termed ER stress results in apoptotic cell death, involving nuclear fragmentation,

Address correspondence to Taiichi Katayama, Dept. of Anatomy and Neuroscience, Graduate School of Medicine, Osaka University, Suita, Osaka 565-0871, Japan. Tel.: 81-6-6879-3221. Fax: 81-6-6879-3229. email: katayama@anat2.med.osaka-u.ac.jp; or Yutaka Eguchi, Division of Molecular Genetics, Dept. of Post-Genomics and Disease, Graduate School of Medicine, Osaka University, Suita, Osaka 565-0871, Japan. Tel.: 81-6-6879-3363. Fax: 81-6-6879-3369. email: eguchi@gene.med.osaka-u.ac.jp

Key words: apoptosis; ER stress; caspase-4; Alzheimer's disease; amyloid-β

condensation of chromatin, and shrinkage of the cell body (Imaizumi et al., 2001). Several mechanisms that activate apoptotic signaling pathways have been reported. For example, the UPR increases the transcription of CHOP/ GADD153 (Brewer et al., 1997), which is closely associated with cell death (Zinszner et al., 1998), recruitment of tumor necrosis factor receptor–associated factor 2 (TRAF2) to activated IRE1α induces c-Jun NH$_2$-terminal kinase activation (Urano et al., 2000), or calpain activates downstream caspase cascade (Nakagawa and Yuan, 2000). However, little is known about the precise mechanisms to lead to ER stress-induced cell death in humans.

Activation of caspases, a family of cysteine proteases that cleave substrates at specific aspartate residues, is a central mechanism in the apoptotic cell death process (Salvesen and Dixit, 1997; Thornberry and Lazebnik, 1998). Most of apoptosis-inducing stimuli lead to release of cytochrome c from mitochondria, which binds to Apaf-1 to activate caspase-9 (Li et al., 1997; Zou et al., 1997), one of initiator caspases with a long pro-domain, and then the activated caspase-9 cleaves effector caspases (Li et al., 1997), including caspases 3 and 7 with a relatively short pro-domain, to activate them. Antiapoptotic Bcl-2 family proteins can rescue cells from apoptosis by protecting mitochondria to prevent cytochrome c release (Kluck et al., 1997; Yang et al., 1997). Several initiator caspases are known to be activated upstream of the mitochondrial dysfunction by specific apoptotic stimuli. For example, Fas stimulation can activate caspase-8 (Fernandes-Alnemri et al., 1996; Muzio et al., 1996), which cannot be inhibited by Bcl-2 (Scaffidi et al., 1998). Among 14 known caspases, caspase-12 seems to be involved in signaling pathways specific to ER stress-induced apoptosis (Nakagawa et al., 2000). Pro–caspase-12 is predominantly localized to the ER, and is specifically cleaved by ER stress. Furthermore, caspase-12–deficient mice show a reduced sensitivity to amyloid-β (Aβ), which is found in brains from Alzheimer's patients (Selkoe, 1986) and shown to cause neuronal cytotoxicity (Yankner et al., 1989). Based on these findings, caspase-12 has been suggested to play an important role in the pathogenesis of AD and to represent a potential target of treatment. However, caspase-12 has only been cloned in the mouse and rat so far, and therefore it is controversial whether similar mechanisms operate in humans (Katayama et al., 1999; Rao et al., 2001; Fischer et al., 2002).

Human genome sequence that is highly homologous to mouse caspase-12 has been identified at the locus within the caspase-1/interleukin-1β converting enzyme (ICE) genes cluster on chromosome 11q22.3 (Fischer et al., 2002), but the gene is interrupted by frame shift and premature stop codon, and also has amino acid substitution in the critical site for caspase activity (Fischer et al., 2002). Therefore, human caspase-12 seems to be lost, and the caspases that substitute for caspase-12 to be activated specifically by ER stress have not been identified in humans so far. We described here that human caspase-4 located within the caspase-1/ICE genes cluster shows similar characteristics to mouse caspase-12. The role of the caspase-4 in ER stress-induced apoptosis and Aβ-induced cell death will be discussed.

Results

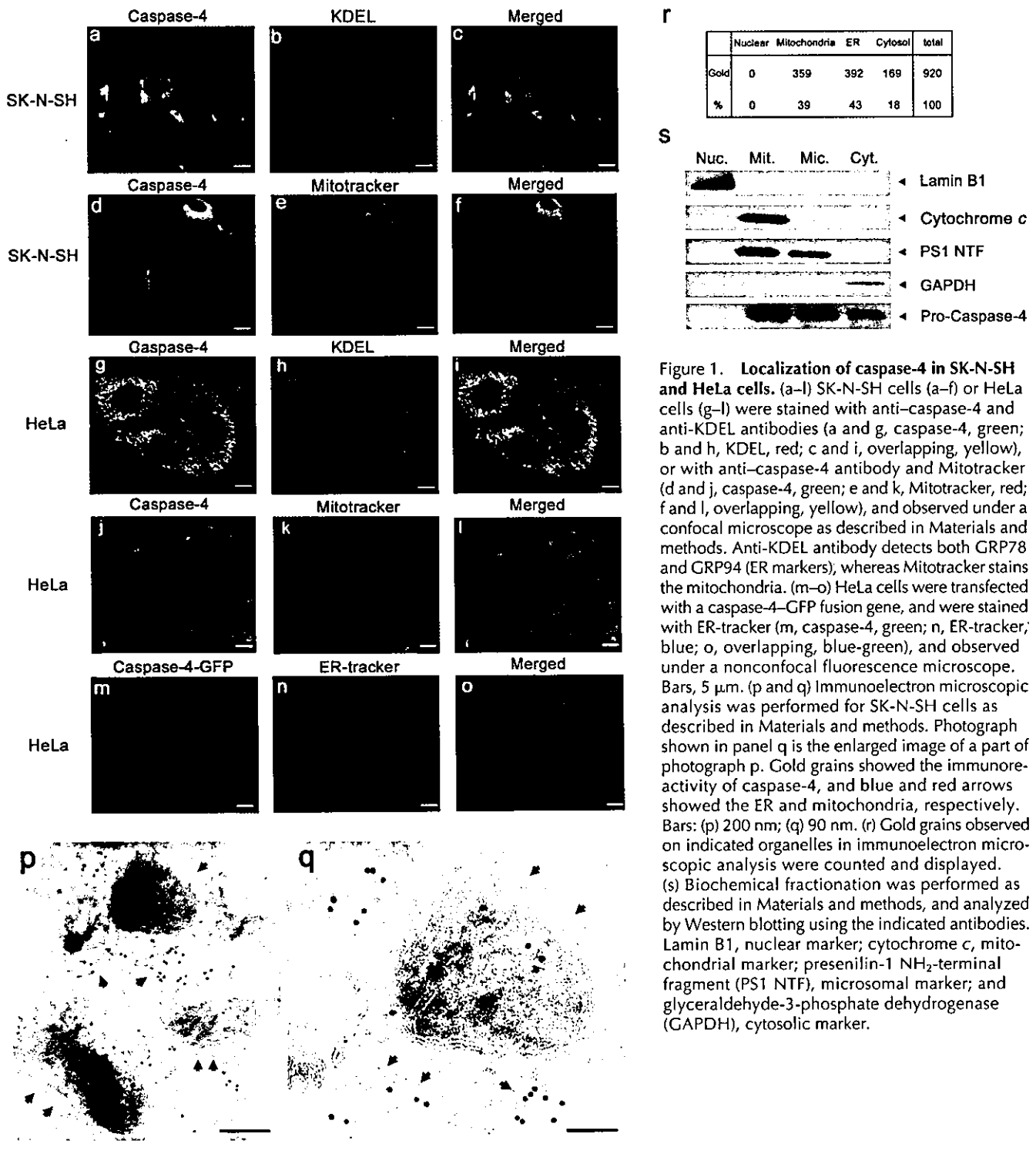## Identification of caspase-4 as a gene homologous to caspase-12

To detect a caspase that was specifically involved in ER stress, we screened human colon cDNA libraries by the plaque hybridization method using the mouse caspase-12 gene as a probe. Human caspase-4 was cloned as the most homologous gene to mouse caspase-12, in agreement with the fact that both molecules belong to the caspase-1/ICE subfamily within the caspase family (Kamens et al., 1995; Lin et al., 2000). Although caspase-5, which has slightly less homology to caspase-12 (caspase-4: 48%; caspase-5: 45%), was also isolated, the screening process yielded much more caspase-4 clones than caspase-5. Because caspase-4 but not caspase-5 was expressed in the cell lines used in this work, which underwent apoptosis in response to ER stress, we assumed that human caspase-4 might functionally substitute for mouse caspase-12 in the human system, and further analyzed the possible role of caspase-4 as a mediator of ER stress-induced apoptosis.

Subcellular localization of caspase-4

First, we studied the subcellular localization of endogenous caspase-4 in SK-N-SH human neuroblastoma cells. Immunofluorescence microscopy showed that immunostaining pattern of caspase-4 strictly overlapped with that of ER markers such as GRP78 and GRP94 (Fig. 1, a–c). Immunoreactivity of caspase-4 was found to overlap only in part with fluorescence signals from Mitotracker (Fig. 1, d–f). These results suggest that caspase-4 was localized predominantly to the ER, and to the mitochondria in addition. The similar results were obtained using HeLa cells (Fig. 1, g–l). When caspase-4 fused with GFP at its COOH terminus was overexpressed in HeLa cells to see the subcellular localization in live cells, most of the fluorescent signals from caspase-4/GFP fusion protein overlapped with those from ER-tracker (Fig. 1, m–o), confirming predominant localization of caspase-4 to the ER by non-immunological method. The immunoelectron microscopic analysis showed that the immunoreactive signals for caspase-4 were found on the ER and mitochondria (Fig. 1, p–r), but much less signals on the nuclei (Fig. 1 r). We also performed biochemical fractionation analysis. Although we could not eliminate contamination of ER marker proteins in the mitochondria-enriched fraction using SK-N-SH cells, probably because we could not disrupt cells homogeneously as the cell line displays heterogeneity in cellular morphology, microsome-enriched fraction does not seem to contain mitochondria and cytosol (Fig. 1 s). Under these conditions, caspase-4 was recovered in both mitochondria-enriched fraction and microsome-enriched fraction, and in cytosolic fraction to a lesser extent (Fig. 1 s), indicating that caspase-4 was surely in microsome-enriched fraction. From these results, we concluded that caspase-4 was localized to the ER, and to the mitochondria in addition, in both SK-N-SH and HeLa cells.

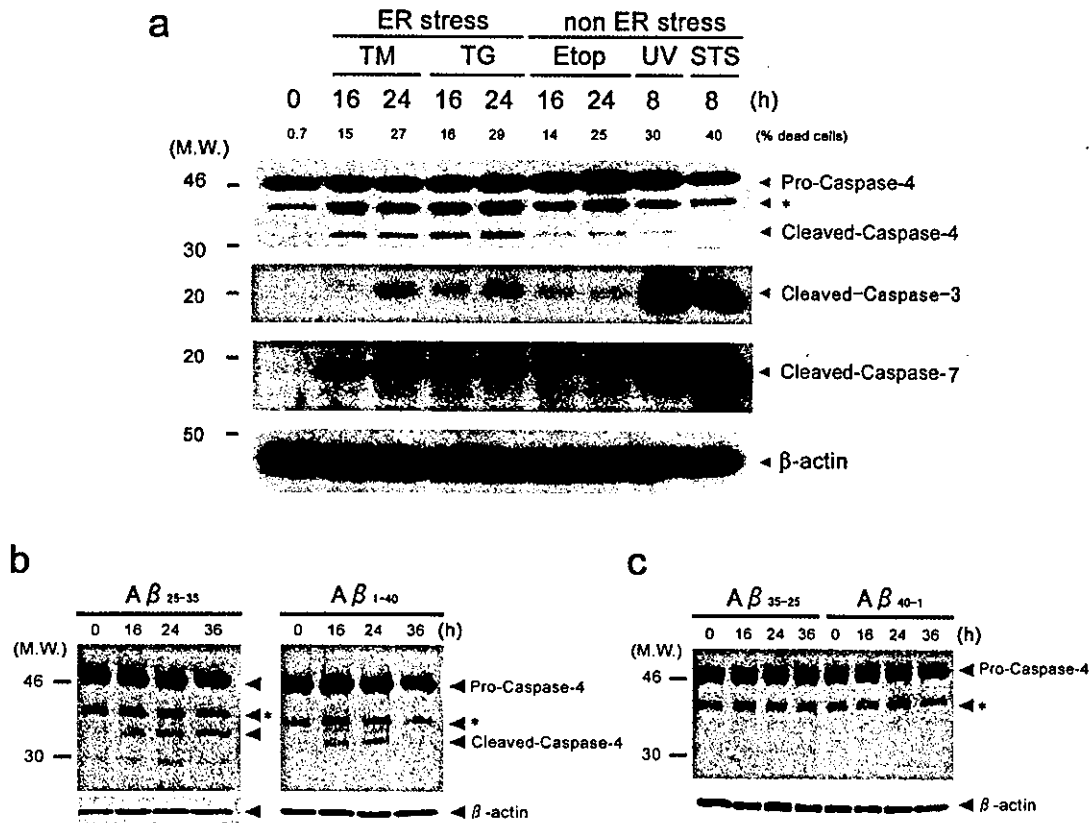## Specific cleavage of caspase-4 by ER stress and Aβ treatments

To examine whether caspase-4 was specifically cleaved by ER stress, we analyzed the cleavage of pro–caspase-4 in re-

r

	Nuclear	Mitochondria	ER	Cytosol	total
Gold	0	359	392	169	920
%	0	39	43	18	100

s

Nuc. Mit. Mic. Cyt.

◄ Lamin B1

◄ Cytochrome c

◄ PS1 NTF

◄ GAPDH

◄ Pro-Caspase-4

Figure 1. Localization of caspase-4 in SK-N-SH and HeLa cells. (a–l) SK-N-SH cells (a–f) or HeLa cells (g–l) were stained with anti–caspase-4 and anti-KDEL antibodies (a and g, caspase-4, green; b and h, KDEL, red; c and i, overlapping, yellow), or with anti–caspase-4 antibody and Mitotracker (d and j, caspase-4, green; e and k, Mitotracker, red; f and l, overlapping, yellow), and observed under a confocal microscope as described in Materials and methods. Anti-KDEL antibody detects both GRP78 and GRP94 (ER markers), whereas Mitotracker stains the mitochondria. (m–o) HeLa cells were transfected with a caspase-4–GFP fusion gene, and were stained with ER-tracker (m, caspase-4, green; n, ER-tracker, blue; o, overlapping, blue-green), and observed under a nonconfocal fluorescence microscope. Bars, 5 μm. (p and q) Immunoelectron microscopic analysis was performed for SK-N-SH cells as described in Materials and methods. Photograph shown in panel q is the enlarged image of a part of photograph p. Gold grains showed the immunore-activity of caspase-4, and blue and red arrows showed the ER and mitochondria, respectively. Bars: (p) 200 nm; (q) 90 nm. (r) Gold grains observed on indicated organelles in immunoelectron microscopic analysis were counted and displayed. (s) Biochemical fractionation was performed as described in Materials and methods, and analyzed by Western blotting using the indicated antibodies. Lamin B1, nuclear marker; cytochrome c, mitochondrial marker; presenilin-1 NH₂-terminal fragment (PS1 NTF), microsomal marker; and glyceraldehyde-3-phosphate dehydrogenase (GAPDH), cytosolic marker.

sponse to several apoptotic stimuli (Fig. 2 a). We found that cleavage of pro–caspase-4 was induced in SK-N-SH cells by treatment with tunicamycin and thapsigargin, both of which caused ER stress. In contrast, when cells were exposed to non-ER stress inducers such as etoposide, staurosporine, and UV at a dose providing similar extent of cell death to that by tunicamycin and thapsigargin, final cleavage products of pro–caspase-4 (Fig. 2 a, cleaved-caspase-4, arrowhead) was not observed. Although the bands shown by the asterisks in Fig. 2 a, which should be derived from

pro–caspase-4 by unknown processing reaction, judging from the data below (Fig. 4 b), were also increased, they were also observed in nontreated cells, so we speculated that the bands were not the final processed form of caspase-4. Under the same conditions, cleavage of caspases 3 and 7, the downstream caspases, was observed regardless of apoptotic stimulations (Fig. 2 a). These results suggest that caspase-4 is specifically activated by apoptotic stimuli inducing ER stress, but not by other stimuli that do not cause ER stress.

Figure 2. **Specific cleavage of caspase-4 by ER stress and Aβ treatment.** (a) SK-N-SH cells were treated with 1 μg/ml tunicamycin (TM), 0.5 μM thapsigargin (TG), 100 μM etoposide (Etop), or 0.1 μM staurosporine (STS) for indicated periods, or irradiated with 150 J/m² UV followed by incubation for indicated periods. Equal amounts of cell lysates (15 μg) were analyzed by Western blotting using anti–caspase-4 antibody (top), anti–caspase-3 antibody (second from top), anti–caspase-7 antibody (third from top), or anti–β-actin antibody (bottom). Positions of pro–caspase-4, cleaved caspase-4, cleaved caspase-3, cleaved caspase-7, and β-actin are indicated. Extent of cell death assessed by MTS assay after incubation for indicated periods are also shown at the top of the gels. (b) SK-N-SH cells were treated with 25 μM synthetic Aβ25-35 or 5 μM Aβ1-40 peptides for the indicated periods. Equal amounts of cell lysates (15 μg) were analyzed by Western blotting using anti–caspase-4 antibody (top) and anti–β-actin antibody (bottom) as a control. Positions of pro–caspase-4, cleaved caspase-4, and β-actin are indicated. (c) SK-N-SH cells were treated with the reverse peptides (25 μM Aβ35-25 and 5 μM Aβ40-1, respectively) for the indicated periods, and cleavage of caspase-4 was examined as in panel b. (a–c) Bands marked by asterisks are likely to be derived from pro–caspase-4 by unknown processing reaction.

To address the possibility that caspase-4 contributes to the mechanism of Aβ-induced cell death in humans, we examined the cleavage of caspase-4 in SK-N-SH cells after treatment with Aβ. When cells were incubated with 25 μM Aβ25-35 or 5 μM Aβ1-40, cleavage of caspase-4 was observed (Fig. 2 b). In contrast, treatment of cells with the reverse peptides (Aβ35-25 and Aβ40-1, respectively), which were not toxic, did not induce the cleavage of caspase-4 (Fig. 2 c). These results suggest that caspase-4 is activated by neurotoxic Aβ treatment similar to ER stress-induced apoptosis.

### Cleavage of caspase-4 in the presence of Bcl-2

To confirm that cleavage of caspase-4 was not due to other caspases activated downstream of the mitochondrial pathway, we examined the effect of overexpression of Bcl-2 and Bcl-xL on apoptosis induced by tunicamycin. Apoptotic nuclear morphological changes were induced by treatment of vector transfectants of SK-N-SH and of HeLa cells with tunicamycin for 30 h, but such changes were completely suppressed by overexpression of Bcl-2 (Fig. 3) or Bcl-xL (not depicted), indicating that the apoptotic signaling pathway

downstream of mitochondria was not operating in cells with overexpression of these antiapoptotic proteins. However, cleavage of caspase-4 after 16 h of tunicamycin treatment was only slightly affected by overexpression of Bcl-2 (Fig. 3) or Bcl-xL (not depicted). These results suggested that caspase-4 is largely activated before the activation of effector caspases during ER stress-induced cell death.

Requirement of caspase-4 for ER stress- and Aβ-induced apoptosis

To determine whether caspase-4 is required for ER stress-induced cell death, SK-N-SH cells that expressed endogenous caspase-4 were transfected with small interfering RNA (siRNA) to caspase-4 or GFP as a control. Immunofluorescence analysis showed that the amount of caspase-4 was substantially decreased by incubation for 60 h after transfection with siRNA directed against caspase-4, but immunoreactivity of caspase-4 was not affected by transfection with GFP-siRNA, when compared with nontransfected cells (Fig. 4 a). Western blot analysis also showed that the amount of caspase-4 was decreased by siRNA to caspase-4 (Fig. 4 b). These re-

a

b
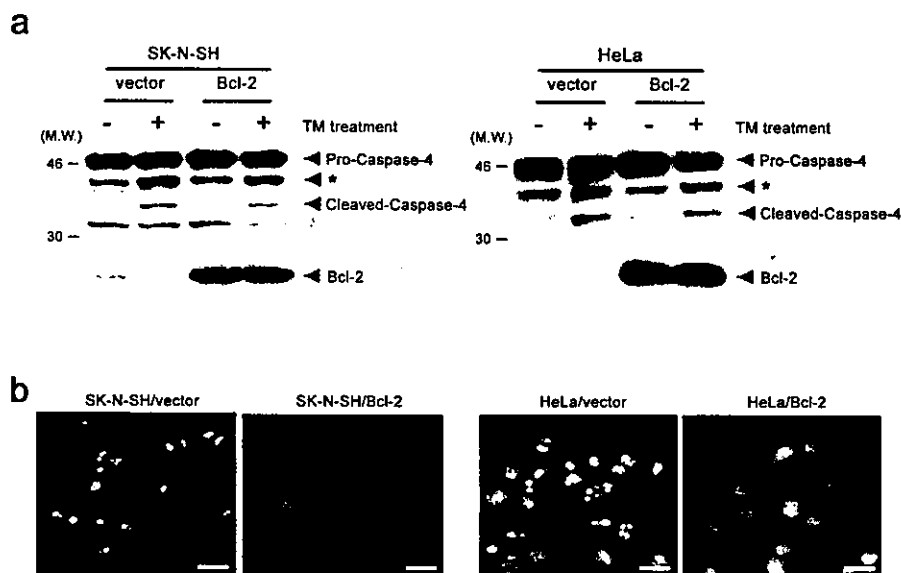
Figure 3. No effect of Bcl-2 overexpression on ER stress-induced cleavage of caspase-4. (a) SK-N-SH cells (left) and HeLa cells (right) stably transfected with the vector or a Bcl-2 expression system were incubated with (+) or without (−) 1 μg/ml tunicamycin for 16 h. Equal amounts of cell lysates were analyzed by Western blotting using anti–caspase-4 antibody (top) and anti–Bcl-2 antibody (bottom). Positions of pro–caspase-4, cleaved caspase-4, and Bcl-2 are indicated. Asterisks show processed caspase-4 as described in Fig. 2 a. (b) The indicated cells were treated with 1 μg/ml tunicamycin for 30 h, stained with Hoechst 33342, and observed under a fluorescence microscope. Bars, 25 μm.

sults showed that the siRNA could diminish the amount of caspase-4, and that the antibody used here specifically recognized caspase-4 in immunohistochemical analysis.

We next examined the effect of decrease in caspase-4 level by siRNA on ER stress-induced apoptosis. Assessment of cell death on the basis of morphological changes showed that ~60% of untransfected SK-N-SH cells were killed by treatment with thapsigargin for 40 h. The extent of cell death was unaffected by transfection with siRNA to GFP (Fig. 4 c). In contrast, only ~30% of the cells died after being transfected with caspase-4 siRNA and exposed to the same stimulation with thapsigargin (Fig. 4 c). As shown in Fig. 4 b, treatment with thapsigargin for 24 h yielded lower level of cleaved-caspase-4 in the cells transfected with caspase-4 siRNA than in the cells transfected with GFP-siRNA. Because the amount of cleaved caspase-4 shown in Fig. 4 b seemed to correlate with the extent of cell death in Fig. 4 c, incomplete inhibition of cell death by transfection with caspase-4 siRNA could be due to residual activity of caspase-4. These results indicate that cells with decreased expression of caspase-4 become more resistant to ER stress-induced cell death.

When cell death was examined by the MTS assay, treatment with caspase-4 siRNA, but not with GFP-siRNA, increased the resistance to ER stress-induced cell death (Fig. 4 d). The increase in the resistance to ER stress-induced cell death was also observed when siRNA to caspase-4 with a different sequence (caspase-4 siRNA-b) was used (Fig. 4 d), indicating that the effect was due to the decreased expression of caspase-4, but not by a specific side effect of caspase-4 siRNA that might affect the expression of other genes. On the other hand, the efficiency of cell death induced by etoposide treatment was not significantly affected by both caspase-4 siRNAs (Fig. 4 d). Therefore, caspase-4 is likely to be specifically involved in ER stress-induced cell death.

To know whether caspase-4 is involved in ER stress-induced cell death in other cell lines, we examined the effect of caspase-4 siRNA using HeLa cells. As shown in Fig. 4 e, treatment of HeLa cells with caspase-4 siRNA significantly increased the resistance to ER stress-induced cell death, although the extent of the increase in resistance was less than

that observed for SK-N-SH cells. This is probably because some other apoptotic mechanisms might also operate simultaneously in HeLa cells. Therefore, we concluded that caspase-4 is likely to be involved in ER stress-induced cell death at least in part in HeLa cells.

We next examined whether caspase-4 is involved in Aβ-induced cell death. When treated with Aβ$_{25-35}$, SK-N-SH cells transfected with caspase-4 siRNA showed significant reduction in cell death compared with the cells transfected with GFP-siRNA (Fig. 4 f). From these results presented here, we concluded that caspase-4 is involved in Aβ-induced cell death, as well as in ER stress-induced cell death.

Discussion

It has been known that apoptotic morphological changes are observed in cell death caused by ER stress (Imaizumi et al., 2001). Caspases are activated to transmit apoptotic signals transcending the difference in species (Alnemri et al., 1996). In rodents, caspase-12 mediates apoptosis specifically in response to ER stress (Nakagawa et al., 2000). Although human caspase-12 gene is transcribed into mRNA, mature caspase-12 protein would not be produced, because the gene is interrupted by frame shift and premature stop codon (Fischer et al., 2002). Furthermore, it contains amino acid substitution in the critical site, which leads to loss of function in several caspases (Fischer et al., 2002). Thus, human caspase-12 does not seem to function in ER stress-induced apoptosis, and some other caspases with similar structure might substitute functionally for caspase-12 in humans. The caspase-12 gene is located within a region where caspase-1/ICE subfamily genes cluster (caspases 1, 4, 5, 12 in human and caspases 1, 11, 12 in mouse). No locus with a comparably high homology to rodent caspase-12 could be found in the human genome. Caspases 4 and 5 are located between caspases 1 and 12 in human genome, whereas only caspase-11 is located between caspases 1 and 12 in mouse. Although it is not known why the region in human genome contains gene duplication, caspases 4 and 5 have been thought to function similarly to caspases 11 and 12. Mouse caspase-11
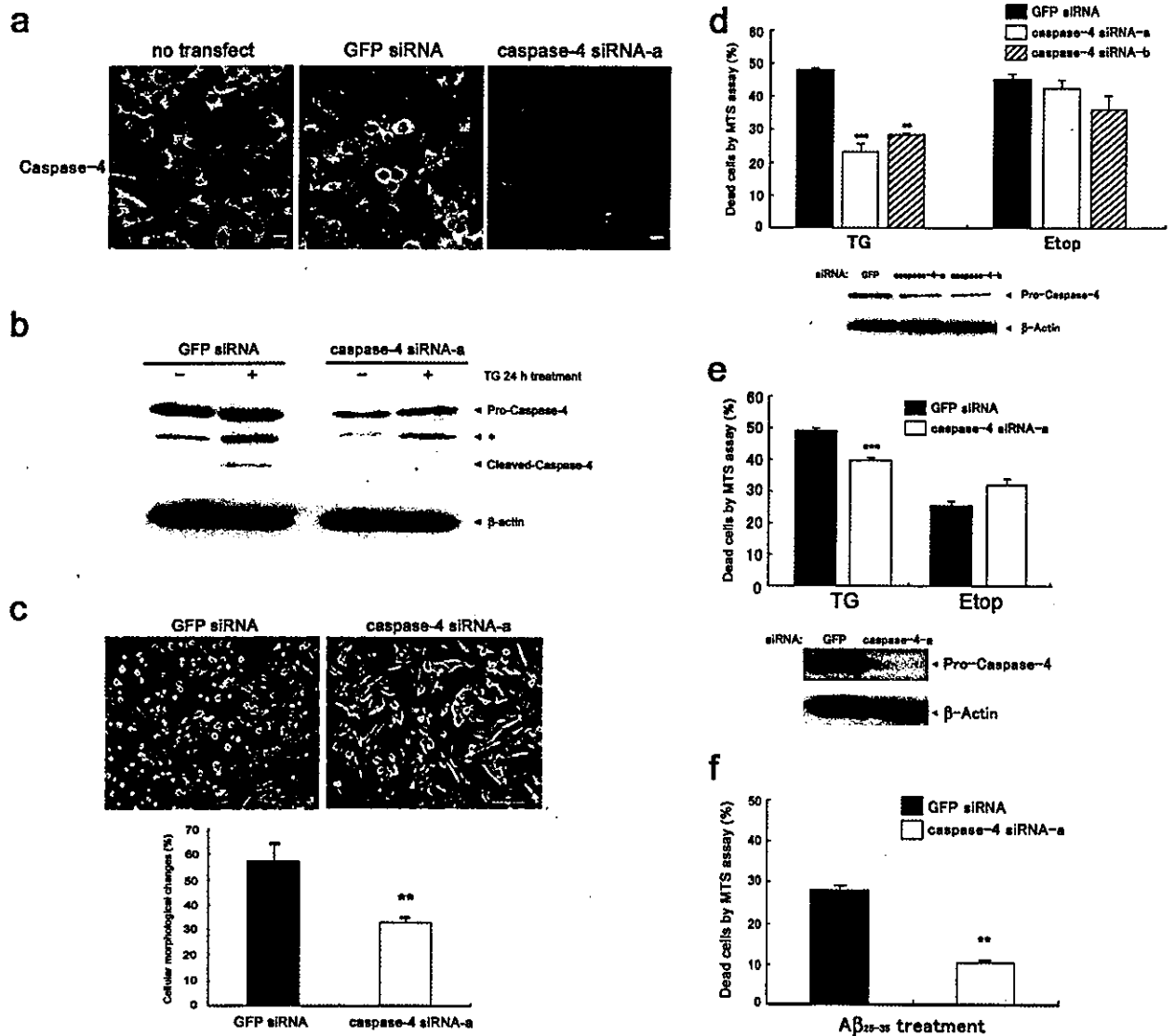
Figure 4. **Decrease in ER stress- or Aβ-induced cell death after siRNA-mediated reduction of caspase-4 expression.** (a) SK-N-SH cells were transfected with siRNA oligos (1 μg oligo/24 well plate) to GFP (control) or caspase-4 (siRNA-a). After incubation for 60 h, cells were fixed and stained with caspase-4 antibodies as described in Materials and methods. Bars, 5 μm. (b) Cells were transfected as in panel a. After incubation for 60 h, cells were incubated with (+) or without (−) 0.5 μM thapsigargin for 24 h. Equal amounts of cell lysates (10 μg) were analyzed by Western blotting using anti–caspase-4 antibody (top) or anti–β-actin antibody (bottom). (c) Top panels show representative phase-contrast images of GFP siRNA-transfected cells (left) and caspase-4 siRNA-a-transfected cells (right) after treatment with 0.5 μM thapsigargin for 40 h. The bottom panel shows the extent of cell death assessed by morphological changes, and expressed as the mean ± SEM for three independent experiments as described in Materials and methods. Asterisks show a significant difference from controls (GFP siRNA-transfected cells): **, indicates P < 0.01. Bars, 50 μm. (d) Cells were transfected with the indicated siRNAs, and cell viability after 0.5 μM thapsigargin or 100 μM etoposide treatment for 40 h was estimated by the MTS assay. Results were expressed as the mean ± SEM for three independent experiments. Asterisks show a significant difference from controls: **, indicates P < 0.01; ***, indicates P < 0.001. Bottom panel shows reduction of caspase-4 level by the indicated siRNAs assessed by Western blotting as described in panel b. (e) HeLa cells were transfected with GFP siRNA or caspase-4 siRNA-a as described in Materials and methods. After incubation for 24 h, cells were incubated with 0.5 μM thapsigargin for 40 h, and then viability was estimated as described in panel d. Each value represents the mean ± SEM for three independent experiments. Asterisks show a significant difference from controls: ***, indicates P < 0.001. (f) SK-N-SH cells were transfected with GFP siRNA or caspase-4 siRNA-a. After incubation for 60 h, cells were incubated with 25 μM Aβ25-35 peptide for 40 h, and then viability was estimated as described in panel d. Each value represents the mean ± SEM for three independent experiments. Asterisks show a significant difference from controls: **, indicates P < 0.01.

is essential for the activation of caspase-1/ICE to promote pro–IL-1β (interleukin-1β) processing (Wang et al., 1996, 1998). On the other hand, caspase-5 is likely involved in processing of pro–IL-1β together with caspase-1/ICE (Martinon et al., 2002) and the caspase-5 gene resembles the mouse caspase-11 in its lipopolysaccharide inducibility (Lin et al., 2000). Therefore, caspase-5 should be the orthologue of caspase-11. Here, the screening process yielded the caspase-4 gene as the homologous gene to mouse caspase-12. Thus, caspase-4 is the best candidate that would function similarly to mouse caspase-12 in ER stress-induced cell death in humans.

Here, we examined the localization of human caspase-4 using several methods. The immunostaining analysis using anti–caspase-4 antibody and fluorescent analysis for caspase-4/GFP fusion protein in Fig. 1 showed the predominant localization of caspase-4 on the ER. On the other hand, the immuno-EM showed the nearly equal distribution of caspase-4 on the ER and mitochondria, and subcellular fractionation showed that caspase-4 was recovered in the microsome-enriched and mitochondria-enriched fractions, and also in cytosolic fraction. Although we could not eliminate contamination of ER marker proteins in the mitochondria-enriched fraction in subcellular fractionation using SK-N-SH cells, microsome-enriched fraction does not seem to contain mitochondria and cytosol. Under these conditions, caspase-4 was recovered in both mitochondria-enriched fraction and microsome-enriched fraction, and amounts of caspase-4 recovered in the microsome-enriched and mitochondria-enriched fractions were comparable to those of ER marker, presenilin-1. Therefore, considering all the results shown in Fig. 1, we concluded that caspase-4 was localized to the ER membrane, and probably to the mitochondria in addition.

Caspase-4 on the ER is supposed to function in ER stress-induced apoptosis similarly to caspase-12. In supporting this hypothesis, caspase-4 was cleaved specifically by ER stress and Aβ-treatment, but not by other apoptotic stimuli including etoposide, staurosporine, and UV. Additionally because Bcl-2 that can completely inhibit the signaling pathway at least downstream from mitochondria, did not prevent the cleavage of caspase-4 by ER stress, it should be most probable that caspase-4 on the ER but not on mitochondria is primarily cleaved. We also showed that reduction of the level of caspase-4 by RNA interference (RNAi) resulted in decrease in ER stress-induced cell death and Aβ-induced cell death, but did not affect cell death induced by etoposide. The characteristics of human caspase-4 shown here are very similar to those of mouse caspase-12 reported previously (Nakagawa et al., 2000), and therefore, caspase-4 is able to substitute the caspase-12 functions in ER stress-induced apoptosis and Aβ-induced cell death. Because caspase-4 was also localized to the mitochondria in addition to the ER membrane, whereas caspase-12 was shown to localize predominantly to the ER, but not to the mitochondria (Nakagawa et al., 2000), caspase-4 might have additional function compared with caspase-12, although the function of caspase-4 on mitochondria is not clear.

Several mechanisms that activate caspase-12 have been proposed in mouse system. For example, calpain, a protease that can be activated by calcium released from ER upon ER stress, starts cleavage of caspase-12 (Nakagawa and Yuan, 2000), caspase-7 activates caspase-12 upon prolonged ER stress (Rao et al., 2001), or TRAF2 mediates caspase-12 activation, which is regulated by IRE1α (Yoneda et al., 2001). It is not clear which mechanism is involved in activation of caspase-4, but because final cleavage products were not observed in cells with activated caspase-7 (Fig. 2 a), activation of caspase-7 does not seem to be enough for full activation of caspase-4. To know the precise mechanism that activate caspase-4, it should be important to find proteins that interact with pro–caspase-4 during ER stress-induced apoptosis.

The inhibition of apoptosis induced by ER stress exposure by RNAi to caspase-4 was incomplete. It is possible that the residual activity of caspase-4 after RNAi would be responsible for the cell death. Alternatively, other apoptotic mechanisms might also operate simultaneously. Several possible pathways have been postulated for ER stress-induced apoptosis. ER stress is reported to activate ASK-c-Jun NH₂-terminal kinase pathway through the IRE1–TRAF2–ASK1 complex formation (Nishitoh et al., 2002). Other signaling pathway is mediated by transcriptional activation of genes encoding proapoptotic function. Activation of stress transducer IRE1, PERK, or ATF6 leads to transcriptional activation of CHOP/GADD153, a bZIP transcription factor that potentiates apoptosis (Oyadomari et al., 2002). Operation of these mechanisms might account for incomplete inhibition of ER stress-induced apoptosis by knockout of caspase-12 and knockdown of caspase-4 in mouse and humans, respectively. It is possible that caspase-dependent mechanism and other mechanisms function in parallel in initiating ER stress-induced apoptosis, and the mechanism that mainly operates could differ depending on cell types. We have shown that the extent to decrease in cell death by decreasing caspase-4 level of SK-N-SH cells was comparable to that reported for caspase-12 knockout mouse (Nakagawa et al., 2000), whereas that of HeLa cells was relatively less. We also find some cells, like HUVEC, in which decrease in caspase-4 did not affect the ER stress-induced apoptosis (unpublished data). Thus, caspase-4 has been shown to function in ER stress-induced apoptosis at least in several cell lines, including SK-N-SH and HeLa cells, but not all cells.

Cell death caused by Aβ treatment was also partially inhibited by RNAi to caspase-4. Although it is controversial whether Aβ-induced cell death involves ER stress-induced apoptosis, the results are consistent that these two types of cell death are mediated by common mechanism at least in part. Recent report described that the cell death induced by Aβ was inhibited by the broad-spectrum caspase inhibitor z-VAD and more specifically by the down-regulation of caspase-2 with antisense oligonucleotides (Haviv et al., 1998). Neuronal culture derived from caspase-2 null mice was also shown to be partially resistant to Aβ₁₋₄₂ toxicity (Troy et al., 2000). Thus Aβ₁₋₄₂-induced cell death might be mediated by caspase-2 as well as caspase-12. It is possible that both caspases 2 and 4 are involved in Aβ-induced cell death also in the human system.

Because caspase-4 seems to be responsible for cell death after Aβ treatment, caspase-4 might be involved in pathogenesis of AD. Consistently to this hypothesis, our preliminary analysis showed an increase in cytoplasmic staining for caspase-4 in the pyramidal cell layer of the hippocampal CA1-2 region in AD patients, but not in control brains (unpublished data). All of the AD brains tested had stronger caspase-4 immunoreactivity than disease control brains from patients with other neurodegenerative disorders ($n = 4$ for AD and $n = 3$ for disease control), and the strong staining was remarkable in the pyramidal neurons around deposits of β-amyloid. Increased caspase-4 might elevate the vulnerability of neurons to apoptosis, and therefore may be involved in the pathogenesis of AD.

Bcl-2 family proteins play essential roles in regulating apoptosis. Although antiapoptotic family members (Bcl-2, Bcl-x_L) and multidomain proapoptotic members (Bak, Bax) are thought to function mainly on mitochondria, recent studies suggest that they may also function on the ER where they reside as well. Overexpression of Bcl-2 (Foyouzi-Youssefi et al., 2000; Pinton et al., 2000) or knockout of both Bak and Bax (Scorrano et al., 2003) are reported to reduce ER Ca^{2+} concentration, but other reports showed that Bcl-2 enhanced the retention of Ca^{2+} in the ER lumen (Distelhorst et al., 1996; He et al., 1997). Thus, although it is still controversial, Bcl-2 family members may contribute to regulating ER stress-induced apoptosis on the ER (Ferri and Kroemer, 2001; Scorrano et al., 2003; Zong et al., 2003) in addition to their main function on mitochondria. Our results demonstrate that overexpressed Bcl-2 and Bcl-x_L, which can completely inhibit the signaling pathway at least downstream from mitochondria, did not prevent, but slightly affected, the cleavage of caspase-4 by ER stress. The slight decrease might be due to the absence of its feed back cleavage by downstream effector caspases, such as caspase-3. Therefore, without regard to the mitochondria or the ER where Bcl-2 family functions, activation of caspase-4 should be the primary reaction in ER stress-induced activation of caspases.

In this work, we discovered that caspase-4 plays a key role in ER stress-induced apoptosis in humans. Caspase-4 also seems to act in the β-amyloid–induced cell death, suggesting that human caspase-4 corresponds to rodent caspase-12 to initiate cell death signaling pathway, and that the activation of caspase-4 would mediate neuronal cell death in neurodegenerative disorder. Caspase-4 could be the potential target to develop treatments for such diseases including AD.

Materials and methods

Chemicals and antibodies

We used the following antibodies: anti–caspase-4 mAb (4B9; MBL International Corporation), anti–caspase-4 pAb (Santa Cruz Biotechnology, Inc.), anti-KDEL mAb (10C3; StressGen Biotechnologies), anti–Lamin B1 mAb (L-5; Zymed Laboratories), anti–cytochrome c mAb (7H8.2C12; BD Biosciences), anti–glyceraldehyde-3-phosphate dehydrogenase mAb (6G7; Biogenesis), anti–caspase-3 mAb (19; Transduction), anti–caspase-7 mAb (4G2; MBL International Corporation), anti–β-actin mAb (C4; CHEMICON International Inc.), anti–Bcl-2 mAb (#100; BD Biosciences), Alexa 588–conjugated anti–mouse IgG antibody (Molecular Probes), FITC-conjugated anti–goat IgG antibody (Jackson ImmunoResearch Laboratories), gold-conjugated anti–goat IgG antibody (British BioCell), and HRP-conjugated anti–mouse IgG antibody (Cell Signaling). Anti–presenilin-1 polyclonal antibody was raised by immunizing rabbits with a synthetic peptide corresponding to residues 1–14 of human presenilin-1, and was affinity purified using ProtOn Kit1 (MultiplePeptide Systems). The chemical reagents used in this experiment were tunicamycin, thapsigargin, etoposide, staurosporine (Sigma-Aldrich), and ER-tracker and Mitotracker (Molecular Probes). Cytotoxic peptides, $Aβ_{25-35}$ and $Aβ_{1-40}$, and their reverse peptides, $Aβ_{35-25}$ and $Aβ_{40-1}$, were purchased from Sigma-Aldrich.

Cell culture

Human neuroblastoma SK-N-SH cells and human carcinoma HeLa cells were respectively cultured in α-MEM (Invitrogen) and DME (Invitrogen) both containing 10% FBS, at 37°C under 5% CO_2. For some experiments, these cells were stably transfected with pCAGGS-hBcl-2 (Iwahashi et al., 1997) and pCAGGS-hBcl-x_L (Tagami et al., 2000) to overexpress Bcl-2 and Bcl-x_L, respectively.

cDNA cloning

A human colon cDNA library (Stratagene) was used for hybridization to isolated cDNA homologous to the partial sequence of mouse caspase-12 gene.

Immunofluorescence microscopy

SK-N-SH cells or HeLa cells were incubated with or without Mitotracker probes, and were fixed with 0.1 M phosphate buffer containing 4% PFA for 2 h at 4°C. Cells were incubated with anti–caspase-4 pAb with or without anti-KDEL mAb, followed by FITC- and Alexa 588–conjugated secondary antibodies, respectively. Stained cells were observed under a confocal microscope (model LSM510; Carl Zeiss MicroImaging, Inc.). To determine localization of caspase-4 in live cells, HeLa cells were transfected with caspase-4/GFP fusion gene subcloned into a pcDNA3.1 (Invitrogen) to produce caspase-4 fused with GFP at its COOH terminus, and after 24 h, cells were incubated with ER-tracker probe for 30 min, followed by observation under a fluorescence microscope (model IX71; Olympus).

Immuno-EM

Immuno-EM was performed essentially as described previously (Miyake et al., 2002). In brief, SK-N-SH cells cultured on a 15-cm dish were fixed with 4% PFA in PBS, pH 7.2, at RT for several hours. After harvesting the cells, they were washed with 30 mM Hepes buffer, pH 7.4, several times. The cells were resuspended in 10% gelatin in 30 mM Hepes buffer, pH 7.4, at 37°C. After centrifugation to recover cells, gelatin was solidified on ice. Blocks for ultracryotomy were prepared and infused with 20% polyvinylpyrrolidone/1.84 M sucrose overnight at 4°C. Ultrathin sections were collected on nickel grids and immunostained with anti–caspase-4 pAb. The sections were incubated with gold-conjugated anti–goat IgG antibody (gold particles, 10-nm diam) for 1 h at RT. Grids were contracted in 2% uranyl acetate and examined on a transmission electron microscope (model CM10; Philips).

Subcellular fractionation

SK-N-SH cells cultured on a 15-cm dish were washed twice with PBS, harvested, and suspended in buffer A (50 mM Tris-HCl, pH 8.0, 1 mM EDTA, 0.32 M sucrose, 0.1 mM PMSF) for 5 min on ice. Then the cells were passed through a 25-gauge needle 13 times and centrifuged at 500 g for 10 min to collect a crude nuclear pellet. The supernatant was centrifuged at 1,200 g for 10 min to yield a mitochondria-enriched pellet, which contained mitochondria and microsome as shown in Fig. 1 s. This supernatant was further centrifuged at 100,000 g for 60 min to yield a microsomal pellet and a cytosolic fraction. All of the pellets were dissolved in buffer A containing 1% SDS. Equal volume of each fraction was subjected to Western blotting as described below, using indicated antibodies.

Western blot analysis

Cells treated with the indicated reagents were washed with PBS, harvested, and lysed in TNE buffer (10 mM Tris-HCl, pH 7.8, 1 mM EDTA, 150 mM NaCl, 1 mM PMSF) containing 0.5% NP-40. Equal amounts of protein were subjected to 12% SDS-PAGE and transferred to a PVDF membrane (Millipore). The membrane was blocked with 5% BSA and was incubated with each primary antibody, followed by incubation with an HRP-conjugated secondary antibody. Proteins were visualized with an ECL detection system (Amersham Biosciences).

Preparation and transfection of siRNAs

The annealed double-stranded siRNAs listed below were obtained from Dharmacon, and were used to decrease expression of caspase-4. Caspase-4 siRNA-a: 5'-AAGUGGCCUCUUCACAGUCAUdTdT-3' (sense), 5'-AAAUGACUGUGAAGAGGCCACdTdT-3' (antisense); caspase-4 siRNA-b: 5'-AAGAUUUCCUCACUGGUGUUUdTdT-3' (sense), 5'-AAAAACAC-CAGTGAGGAAATCdTdT-3' (antisense). For control, siRNA to GFP was used. GFP siRNA: 5'-P-GGCUACGUCCAGGAGCGCACC-3' (sense), 5'-P-UGCGCUCCUGGACGUAGCCUU-3' (antisense). These sequences were not significantly homologous to genes other than caspase-4 or GFP by BLAST search (NCBI). SK-N-SH cells were transfected at 50% confluence in 24-well plastic plates with 1.0 μg of each of the above siRNAs using Transmessenger transfection reagent (QIAGEN) according to the manufacturer's protocol. Transfected cells were incubated at 37°C for 60 h without changing the medium. siRNAs were introduced into HeLa cells by electroporation three times with 48-h intervals using Amaxa system according to the manufacturer's protocol. Efficiency of RNAi was measured by immunocytochemical analysis and Western blot analysis using anti–caspase-4 antibody or anti–β-actin antibody.

Cell viability assay

SK-N-SH cells or HeLa cells overexpressing Bcl-2 and Bcl-x_L, or transfected with siRNAs as above were treated with various reagents as indicated. When using $Aβ_{1-40}$, it was preincubated for 1 wk at 37°C to establish its cytotoxicity. Cell death was assessed on the basis of cellular morpho-

logical changes observed by phase-contrast microscopy or from nuclear morphological changes detected by fluorescence microscopy after staining the cells with 10 μM Hoechst 33342. At least 500 cells were counted, and the data was expressed as the mean ± SEM from three independent experiments and P values were calculated by t test. The MTS ([3-(4, 5-dimethylthiazol-2-yl)-5-(3-carboxymethoxyphenyl)-2-(4-sulfophenyl)-2H-tetrazolium, inner salt]) assay was also performed to evaluate cell viability. After treatment with apoptosis-inducing reagents, cells were coincubated with MTS solution (Promega) for 1 h at 37°C. The amount of reduced MTS released from the viable cells was quantified by measuring the absorbance at 490 nm using a spectrophotometer. Results were expressed as a ratio (%) of dead cells after treatments to those in control as above.

References

Alnemri, E.S., D.J. Livingston, D.W. Nicholson, G. Salvesen, N.A. Thornberry, W.W. Wong, and J. Yuan. 1996. Human ICE/CED-3 protease nomenclature. *Cell.* 87:171.

Bonifacino, J.S., and A.M. Weissman. 1998. Ubiquitin and the control of protein fate in the secretory and endocytic pathways. *Annu. Rev. Cell Dev. Biol.* 14: 19–57.

Brewer, J.W., J.L. Cleveland, and L.M. Hendershot. 1997. A pathway distinct from the mammalian unfolded protein response regulates expression of endoplasmic reticulum chaperones in non-stressed cells. *EMBO J.* 16:7207–7216.

Distelhorst, C.W., M. Lam, and T.S. McCormick. 1996. Bcl-2 inhibits hydrogen peroxide-induced ER Ca^{2+} pool depletion. *Oncogene.* 12:2051–2055.

Fernandes-Alnemri, T., R.C. Armstrong, J. Krebs, S.M. Srinivasula, L. Wang, F. Bullrich, L.C. Fritz, J.A. Trapani, K.J. Tomaselli, G. Litwack, and E.S. Alnemri. 1996. In vitro activation of CPP32 and Mch3 by Mch4, a novel human apoptotic cysteine protease containing two FADD-like domains. *Proc. Natl. Acad. Sci. USA.* 93:7464–7469.

Ferri, K.F., and G. Kroemer. 2001. Organelle-specific initiation of cell death pathways. *Nat. Cell Biol.* 3:E255–E263.

Fischer, H., U. Koenig, L. Eckhart, and E. Tschachler. 2002. Human caspase 12 has acquired deleterious mutations. *Biochem. Biophys. Res. Commun.* 293: 722–772.

Forman, M.S., V.M. Lee, and J.Q. Trojanowski. 2003. 'Unfolding' pathways in neurodegenerative disease. *Trends Neurosci.* 26:407–410.

Foyouzi-Youssefi, R., S. Arnaudeau, C. Borner, W.L. Kelley, J. Tschopp, D.P. Lew, N. Demaurex, and K.H. Krause. 2000. Bcl-2 decreases the free Ca^{2+} concentration within the endoplasmic reticulum. *Proc. Natl. Acad. Sci. USA.* 97:5723–5728.

Harding, H.P., Y. Zhang, and D. Ron. 1999. Protein translation and folding are coupled by an endoplasmic-reticulum-resident kinase. *Nature.* 397:271–274.

Haviv, R., L. Lindenboim, J. Yuan, and R. Stein. 1998. Need for caspase-2 in apoptosis of growth-factor-deprived PC12 cells. *J. Neurosci. Res.* 52:491–497.

He, H., M. Lam, T.S. McCormick, and C.W. Distelhorst. 1997. Maintenance of calcium homeostasis in the endoplasmic reticulum by Bcl-2. *J. Cell Biol.* 138:1219–1228.

Imai, Y., M. Soda, and R. Takahashi. 2000. Parkin suppresses unfolded protein stress-induced cell death through its E3 ubiquitin-protein ligase activity. *J. Biol. Chem.* 275:35661–35664.

Imai, Y., M. Soda, H. Inoue, N. Hattori, Y. Mizuno, and R. Takahashi. 2001. An unfolded putative transmembrane polypeptide, which can lead to endoplasmic reticulum stress, is a substrate of Parkin. *Cell.* 105:891–902.

Imaizumi, K., K. Miyoshi, T. Katayama, T. Yoneda, M. Taniguchi, T. Kudo, and M. Tohyama. 2001. The unfolded protein response and Alzheimer's disease. *Biochim. Biophys. Acta.* 1536:85–96.

Iwahashi, H., Y. Eguchi, N. Yasuhara, T. Hanafusa, Y. Matsuzawa, and Y. Tsujimoto. 1997. Synergistic anti-apoptotic activity between Bcl-2 and SMN implicated in spinal muscular atrophy. *Nature.* 390:413–417.

Kamens, J., M. Paskind, M. Hugunin, R.V. Talanian, H. Allen, D. Banach, N. Bump, M. Hackett, C.G. Johnston, P. Li, et al. 1995. Identification and characterization of ICH-2, a novel member of the interleukin-1 beta-converting enzyme family of cysteine proteases. *J. Biol. Chem.* 270:15250–15256.

Katayama, T., K. Imaizumi, N. Sato, K. Miyoshi, T. Kudo, J. Hitomi, T. Morihara, T. Yoneda, F. Gomi, Y. Mori, et al. 1999. Presenilin-1 mutations downregulate the signaling pathway of the unfolded-protein response. *Nat. Cell Biol.* 1:479–485.

Kaufman, R.J. 2002. Orchestrating the unfolded protein response in health and disease. *J. Clin. Invest.* 110:1389–1398.

Kluck, R.M., E. Bossy-Wetzel, D.R. Green, and D.D. Newmeyer. 1997. The release of cytochrome c from mitochondria: a primary site for Bcl-2 regulation of apoptosis. *Science.* 275:1132–1136.

Kozutsumi, Y., M. Segal, K. Normington, M.J. Gething, and J. Sambrook. 1988. The presence of malfolded proteins in the endoplasmic reticulum signals the induction of glucose-regulated proteins. *Nature.* 332:462–464.

Li, P., D. Nijhawan, I. Budihardjo, S.M. Srinivasula, M. Ahmad, E.S. Alnemri, and X. Wang. 1997. Cytochrome c and dATP-dependent formation of Apaf-1/caspase-9 complex initiates an apoptotic protease cascade. *Cell.* 91: 479–489.

Lin, X.Y., M.S. Choi, and A.G. Porter. 2000. Expression analysis of the human caspase-1 subfamily reveals specific regulation of the CASP5 gene by lipopolysaccharide and interferon-gamma. *J. Biol. Chem.* 275:39920–39926.

Martinon, F., K. Burns, and J. Tschopp. 2002. The inflammasome: a molecular platform triggering activation of inflammatory caspases and processing of proIL-beta. *Mol. Cell.* 10:417–426.

Miyake, S., T. Yamashita, M. Taniguchi, M. Tamatani, K. Sato, and M. Tohyama. 2002. Identification and characterization of a novel mitochondrial tricarboxylate carrier. *Biochem. Biophys. Res. Commun.* 295:463–468.

Muzio, M., A.M. Chinnaiyan, F.C. Kischkel, K. O'Rourke, A. Shevchenko, J. Ni, C. Scaffidi, J.D. Bretz, M. Zhang, R. Gentz, et al. 1996. FLICE, a novel FADD-homologous ICE/CED-3-like protease, is recruited to the CD95 (Fas/APO-1) death-inducing signaling complex. *Cell.* 85:817–827.

Nakagawa, T., and J. Yuan. 2000. Cross-talk between two cysteine protease families. Activation of caspase-12 by calpain in apoptosis. *J. Cell Biol.* 150:887–894.

Nakagawa, T., H. Zhu, N. Morishima, E. Li, J. Xu, B.A. Yankner, and J. Yuan. 2000. Caspase-12 mediates endoplasmic-reticulum-specific apoptosis and cytotoxicity by amyloid-beta. *Nature.* 403:98–103.

Nishitoh, H., A. Matsuzawa, K. Tobiume, K. Saegusa, K. Takeda, K. Inoue, S. Hori, A. Kakizuka, and H. Ichijo. 2002. ASK1 is essential for endoplasmic reticulum stress-induced neuronal cell death triggered by expanded polyglutamine repeats. *Genes Dev.* 16:1345–1355.

Oyadomari, S., E. Araki, and M. Mori. 2002. Endoplasmic reticulum stress-mediated apoptosis in pancreatic beta-cells. *Apoptosis.* 7:335–345.

Pinton, P., D. Ferrari, P. Magalhaes, K. Schulze-Osthoff, F. Di Virgilio, T. Pozzan, and R. Rizzuto. 2000. Reduced loading of intracellular Ca$^{(2+)}$ stores and downregulation of capacitative Ca$^{(2+)}$ influx in Bcl-2-overexpressing cells. *J. Cell Biol.* 148:857–862.

Rao, R.V., E. Hermel, S. Castro-Obregon, G. del Rio, L.M. Ellerby, H.M. Ellerby, and D.E. Bredesen. 2001. Coupling endoplasmic reticulum stress to the cell death program. Mechanism of caspase activation. *J. Biol. Chem.* 276:33869–33874.

Salvesen, G.S., and V.M. Dixit. 1997. Caspases: intracellular signaling by proteolysis. *Cell.* 91:443–446.

Sato, N., K. Imaizumi, T. Manabe, M. Taniguchi, J. Hitomi, T. Katayama, T. Yoneda, T. Morihara, Y. Yasuda, T. Takagi, et al. 2001. Increased production of beta-amyloid and vulnerability to endoplasmic reticulum stress by an aberrant spliced form of presenilin 2. *J. Biol. Chem.* 276:2108–2114.

Scaffidi, C., S. Fulda, A. Srinivasan, C. Friesen, F. Li, K.J. Tomaselli, K.M. Debatin, P.H. Krammer, and M.E. Peter. 1998. Two CD95 (APO-1/Fas) signaling pathways. *EMBO J.* 17:1675–1687.

Scorrano, L., S.A. Oakes, J.T. Opferman, E.H. Cheng, M.D. Sorcinelli, T. Pozzan, and S.J. Korsmeyer. 2003. BAX and BAK regulation of endoplasmic reticulum Ca^{2+}: a control point for apoptosis. *Science.* 300:135–139.

Selkoe, D.J. 1986. Altered structural proteins in plaques and tangles: what do they tell us about the biology of Alzheimer's disease? *Neurobiol. Aging.* 7:425–432.

Tagami, S., Y. Eguchi, M. Kinoshita, M. Takeda, and Y. Tsujimoto. 2000. A novel protein, RTN-XS, interacts with both Bcl-XL and Bcl-2 on endoplasmic reticulum and reduces their anti-apoptotic activity. *Oncogene.* 19:5736–5746.

Tamatani, M., T. Matsuyama, A. Yamaguchi, N. Mitsuda, Y. Tsukamoto, M. Taniguchi, Y.H. Che, K. Ozawa, O. Hori, H. Nishimura, et al. 2001. ORP150 protects against hypoxia/ischemia-induced neuronal death. *Nat. Med.* 7:317–323.

Thornberry, N.A., and Y. Lazebnik. 1998. Caspases: enemies within. *Science.* 281: 1312–1316.

Travers, K.J., C.K. Patil, L. Wodicka, D.J. Lockhart, J.S. Weissman, and P. Walter. 2000. Functional and genomic analyses reveal an essential coordina-

tion between the unfolded protein response and ER-associated degradation. *Cell.* 101:249–258.

Troy, C.M., S.A. Rabacchi, W.J. Friedman, T.F. Frappier, K. Brown, and M.L. Shelanski. 2000. Caspase-2 mediates neuronal cell death induced by beta-amyloid. *J. Neurosci.* 20:1386–1392.

Urano, F., X. Wang, A. Bertolotti, Y. Zhang, P. Chung, H.P. Harding, and D. Ron. 2000. Coupling of stress in the ER to activation of JNK protein kinases by transmembrane protein kinase IRE1. *Science.* 287:664–666.

Wang, S., M. Miura, Z. Jung, H. Zhu, V. Gagliardini, L. Shi, A.H. Greenberg, and J. Yuan. 1996. Identification and characterization of Ich-3, a member of the interleukin-1beta converting enzyme (ICE)/Ced-3 family and an upstream regulator of ICE. *J. Biol. Chem.* 271:20580–20587.

Wang, S., M. Miura, Y.K. Jung, H. Zhu, E. Li, and J. Yuan. 1998. Murine caspase-11, an ICE-interacting protease, is essential for the activation of ICE. *Cell.* 92:501–509.

Wigley, W.C., R.P. Fabunmi, M.G. Lee, C.R. Marino, S. Muallem, G.N. DeMartino, and P.J. Thomas. 1999. Dynamic association of proteasomal machinery with the centrosome. *J. Cell Biol.* 145:481–490.

Yang, J., X. Liu, K. Bhalla, C.N. Kim, A.M. Ibrado, J. Cai, T.I. Peng, D.P. Jones,

and X. Wang. 1997. Prevention of apoptosis by Bcl-2: release of cytochrome c from mitochondria blocked. *Science.* 275:1129–1132.

Yankner, B.A., L.R. Dawes, S. Fisher, L. Villa-Komaroff, M.L. Oster-Granite, and R.L. Neve. 1989. Neurotoxicity of a fragment of the amyloid precursor associated with Alzheimer's disease. *Science.* 245:417–420.

Yoneda, T., K. Imaizumi, K. Oono, D. Yui, F. Gomi, T. Katayama, and M. Tohyama. 2001. Activation of caspase-12, an endoplastic reticulum (ER) resident caspase, through tumor necrosis factor receptor-associated factor 2-dependent mechanism in response to the ER stress. *J. Biol. Chem.* 276:13935–13940.

Zinszner, H., M. Kuroda, X. Wang, N. Batchvarova, R.T. Lightfoot, H. Remotti, J.L. Stevens, and D. Ron. 1998. CHOP is implicated in programmed cell death in response to impaired function of the endoplasmic reticulum. *Genes Dev.* 12:982–995.

Zong, W.X., C. Li, G. Hatzivassiliou, T. Lindsten, Q.C. Yu, J. Yuan, and C.B. Thompson. 2003. Bax and Bak can localize to the endoplasmic reticulum to initiate apoptosis. *J. Cell Biol.* 162:59–69.

Zou, H., W.J. Henzel, X. Liu, A. Lutschg, and X. Wang. 1997. Apaf-1, a human protein homologous to *C. elegans* CED-4, participates in cytochrome c-dependent activation of caspase-3. *Cell.* 90:405–413.

Apoptosis induced by endoplasmic reticulum stress depends on activation of caspase-3 via caspase-12

Junichi Hitomi[a,b], Taiichi Katayama[a,b,*], Manabu Taniguchi[a,b], Akiko Honda[c],
Kazunori Imaizumi[d], Masaya Tohyama[a,d]

[a]Department of Anatomy and Neuroscience, Osaka University Medical School, 2-2 Yamadaoka, Suita, Osaka, 565-0871, Japan
[b]Core Research for Evolutional Science and Technology, Japan Science and Technology, Kawaguchi, Saitama, 332-0012, Japan
[c]Tanabe Seiyaku Company Limited, Yodogawaku, Osaka 532-0031, Japan
[d]Department of Cellular and Structural Biology, Graduate School of Biological Sciences, Nara Institute of Science and Technology, 8916-5 Takayama Ikoma, Nara 630-0101, Japan

Received 29 July 2003; received in revised form 14 November 2003; accepted 3 December 2003

Abstract

Recently, endoplasmic reticulum (ER) dysfunction has been implicated in neuronal death in patients with Alzheimer's disease. Treatment of human neuroblastoma cells with ER stress inducers causes apoptotic death. We confirmed that ER stress inducers specifically targeted the ER to cause apoptotic morphological changes. We also found that caspase-3, and not caspase-9 (a known mitochondrial apoptotic mediator), was mainly activated by ER stress. We generated the neuroblastoma cells that stably expressed caspase-12 and analyzed its influence on caspase-3 activation and vulnerability to ER stress. Cells expressing caspase-12 were more vulnerable to ER stress than cells expressing the empty vector, concomitant with increased activation of caspase-3. These findings suggested that activation of ER-resident caspase-12 indirectly activates cytoplasmic caspase-3 and might be important in ER stress-induced neuronal apoptosis.
© 2003 Elsevier Ireland Ltd. All rights reserved.

Keywords: SK-N-SH neuroblastoma cells; Endoplasmic reticulum stress; Apoptosis; Caspase-12; Caspase-3

The endoplasmic reticulum (ER) is an organelle that ensures correct protein folding and assembly by expressing numerous molecular chaperones [3,7]. Under various conditions, such as glucose starvation, disturbance of intracellular calcium homeostasis, inhibition of protein glycosylation, or exposure to free radicals, unfolded proteins accumulate in the ER lumen, a process called ER stress. Excessive ER stress induces cell death [6,17]. Neuronal death in some neurodegenerative disorders, especially Alzheimer's disease (AD), is reported to be due to ER dysfunction. Familial AD-linked presenilin-1 mutants or presenilin-2 splice variants which are expressed in sporadic AD brains, and increase neuronal vulnerability to ER stress [5,13,14]. Thus, the ER may be important for regulating intracellular apoptotic signals in neurons, but the mechanisms of ER stress-induced cell death are poorly understood.

Caspase-12, one of the caspase family of proteases, is localized to the ER and is specifically activated by ER stress [10], with several possible mechanisms being suggested [9, 12,18]. Caspase-12-deficient cells are resistant to ER stress, but not non-ER stress [10], and such evidence suggests that caspase-12 is a major mediator of ER-stress-induced apoptosis.

We found that activation of ER resident caspase-12 causes activation of cytoplasmic caspase-3, and not mitochondria-related caspase-9, during ER stress-induced apoptosis.

When cells die from ER stress, it is believed that apoptosis occurs, but whether these cells show typical morphological features of apoptosis is unclear. Therefore, we analyzed the morphological and biochemical changes during cell death after ER stress in SK-N-SH, human neuroblastoma cells.

a

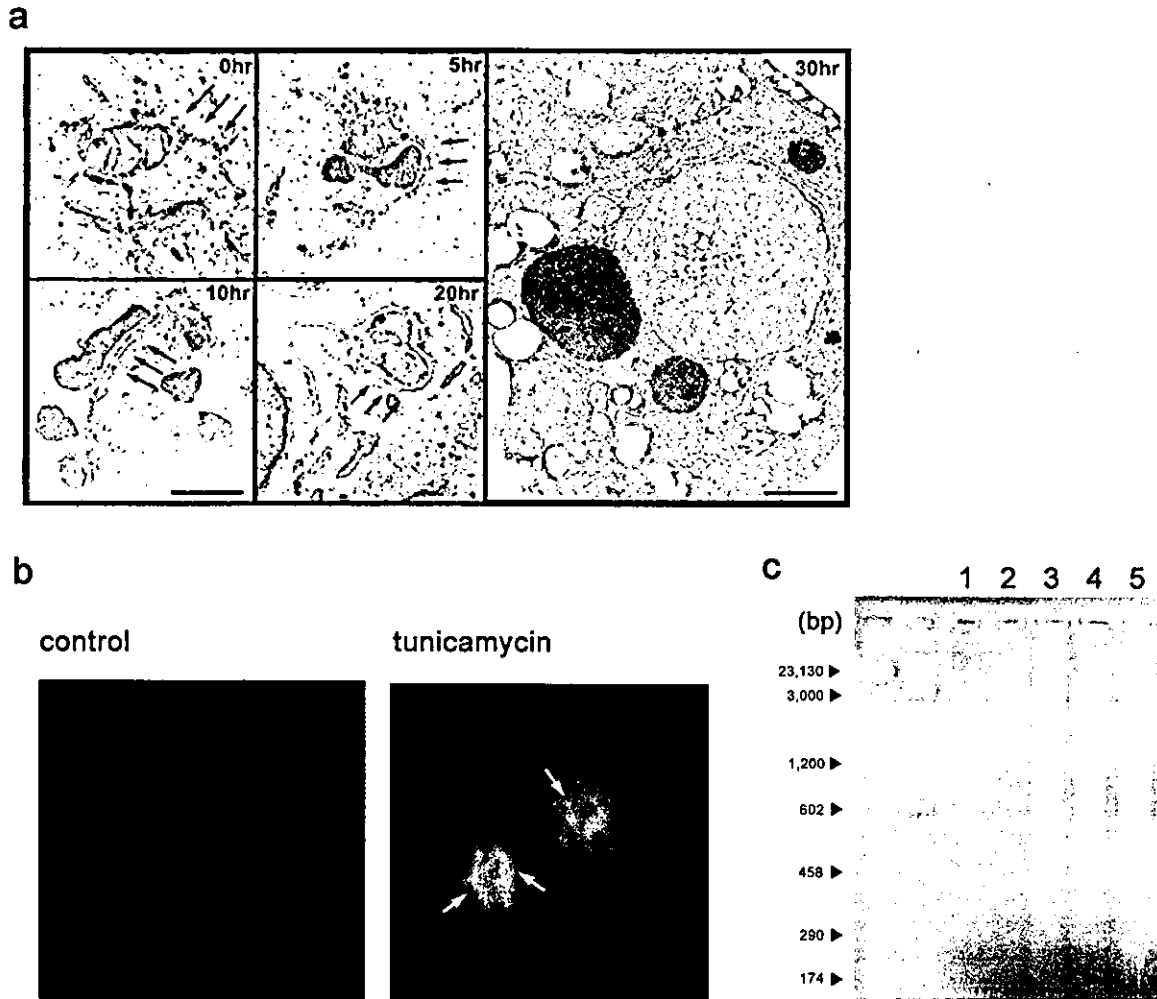b

control   tunicamycin

c

Fig. 1. Morphological and biochemical features of apoptosis induced by ER stress. (a) Electron microscopy shows ER luminal swelling (black arrow), detachment of ribosomes from rough ER, and nuclear fragmentation of SK-N-SH cells after treatment with an ER stress inducer, 1.0 μg/ml tunicamycin (Tm). ER luminal swelling occurred before nuclear fragmentation Scale bars represent 1 μm. (b) Hoechst 33258 staining of cells with or without exposure to 1.0 μg/ml Tm for 24 h. White arrows indicate chromatin condensation. (c) DNA laddering in cells treated with 1.0 μg/ml Tm (lane 3) and 0.5 μM Tg (lane 4) for 24 h or 0.1 μM staurosporine (lane 5) for 8 h. Data are representative results from three separate experiments.

As shown in Fig. 1, chronic ER stress (30 h of exposure to 1 μg/ml tunicamycin (Tm), a N-linked glycosylation inhibitor) caused apoptotic morphological changes, including nuclear fragmentation, chromatin condensation, and cell shrinkage. Interestingly, prior to these changes, swelling of the ER lumen and dissociation of ribosomes from rough ER were observed by electron microscopy.

These studies indicated that ER stress-induced cell death was a type of apoptosis.

Caspases are critical mediators of apoptosis in mammalian cells [16], so we measured several caspases activities using synthetic fluorometric substrates (50 μM Ac-YVAD-AMC, Ac-DEVD-AMC, Ac-VEID-AMC, Ac-IETD-AMC, and Ac-LEHD-AMC for caspase-1, caspase-3, caspase-6, caspase-8, and caspase-9, respectively). After 24 h of treatment with 1 μg/ml Tm or 0.5 μM thapsigargin (Tg), an ER Ca^{2+}-ATPase inhibitor, caspase-3 activity was significantly higher than that of other caspases (Fig. 2a, upper).

Activation of caspases requires cleavage of pro-caspases, e.g. pro-caspase-3 is cleaved into smaller subunits under apoptotic conditions [1]. To confirm the role of caspase-3 in ER stress-induced apoptosis, we assessed pro-caspase-3 cleavage in SK-N-SH cells treated with 1 μg/ml Tm by western blotting using an anti-caspase-3 antibody that detected both uncleaved and cleaved caspase-3 (Fig. 2a, bottom). Cleaved caspase-3 was observed under ER stress conditions. Next, we examined the effects of specific caspase inhibitors on apoptosis (Fig. 2b). After exposure to 1 μg/ml Tm with or without each caspase inhibitor (5 μM), cell death was quantified from LDH release into the medium. When cells were treated with both Tm and a caspase-3 inhibitor, death was significantly reduced, suggesting that caspase-3 was a major caspase activated by ER stress. Similar results were observed after treatment with Tg (Fig. 2b, right).
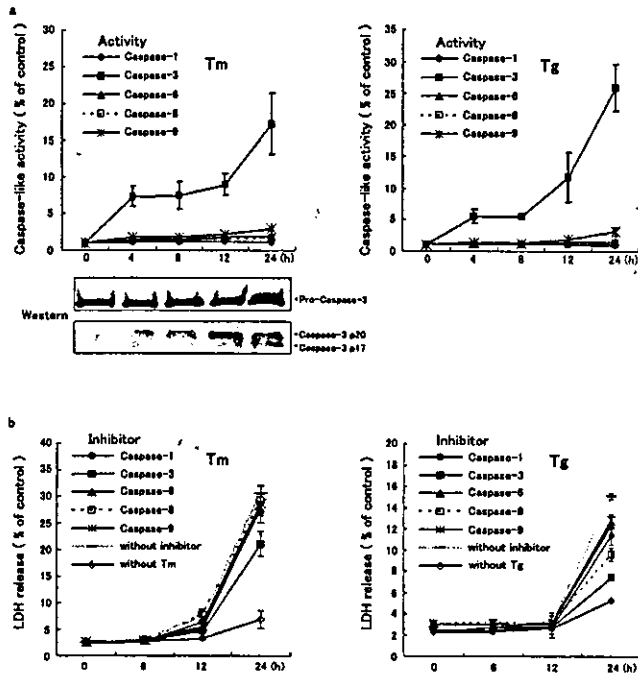
To clarify the link between activation of ER resident

Fig. 2. Caspase-3 activation by ER stress. (a) SK-N-SH cell lysates (50 μg) treated with 1.0 μg/ml Tm or 0.5 μM Tg were incubated with 50 μM Ac-YVAD-AMC (caspase-1, closed circles), Ac-DEVD-AMC (caspase-3, closed squares), Ac-VEID-AMC (caspase-6, closed triangles), Ac-IETD-AMC (caspase-8, open squares), or Ac-LEHD-AMC (caspase-9, asterisks) fluorometric substrates at 37 °C for 30 min and caspase activity was measured using a spectrophotometer with excitation at 380 nm and emission at 460 nm (upper panel). Cytosol was immunoblotted with anti-caspase-3 recognizing both uncleaved and active forms (p20, p17) after treatment with 1.0 μg/ml Tm (bottom panel). (b) To confirm the effect of caspase-3 on death of SK-N-SH cells treated for 24 h with 1.0 μg/ml Tm and 5 μM of each caspase inhibitor [Ac-YVAD-CHO (caspase-1, closed circles), Ac-DEVD-CHO (caspase-3, closed squares), Ac-VEID-CHO (caspase-6, closed triangles), Ac-IETD-CHO (caspase-8, open squares), or Ac-LEHD-CHO (caspase-9, asterisks)], culture medium was collected to assay LDH. Data are mean values from four independent experiments.

caspase-12 and cytoplasmic caspase-3, we assessed caspase-3 activation in SK-N-SH cells with stable expression of caspase-12 or empty vector (mock). Caspase-3 activation was significantly greater in caspase-12-expressing cells than in mock-expressing cells after treatment with 1 μg/ml Tm for 10 h (Fig. 3a). Cleavage of pro-caspase-3 was also increased in caspase-12-expressing cells (Fig. 3a). To investigate whether increased caspase-3 activation in caspase-12-expressing cells was accompanied by vulnerability to ER stress, we compared LDH release by caspase-12- and mock-expressing cells after treatment with 1 μg/ml Tm. Overexpression of caspase-12 increased the vulnerability of cells to Tm (Fig. 3b). To determine whether activated caspase-12 could directly cleave pro-caspase-3, we performed an in vitro cleavage assay using recombinant active caspase-12 [8,10], but found no cleavage of in vitro-translated pro-caspase-3 by recombinant caspase-12 (data not shown). These results suggested that activated caspase-12 might indirectly activate cytoplasmic caspase-3 during ER stress.
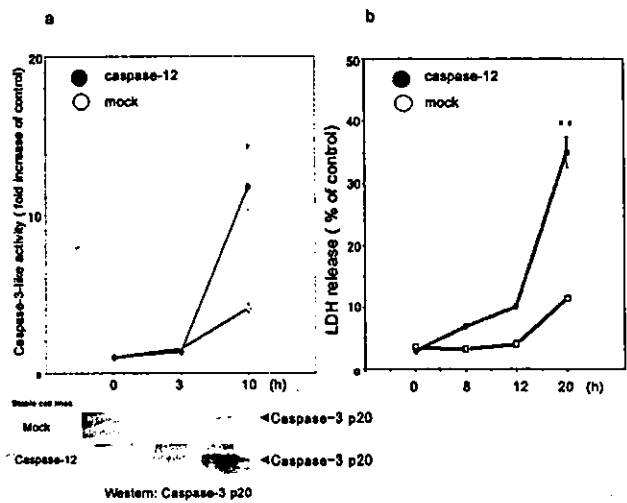

Fig. 3. Caspase-12 overexpressing neuroblastoma cells activate caspase-3 and potentiate vulnerability to ER stress. (a) Increase of caspase-3 activation in cells stably expressing caspase-12 compared with mock (empty vector)-expressing cells. SK-N-SH cells expressing caspase-12 (closed circles) or mock vector (open circles) were treated with 1.0 μg/ml Tm for 20 h and lysed with ICE buffer (50 mM Tris–HCl, pH 7.4, 1 mM EDTA 1 mM EGTA, and 10 μM digitonin). Equal amounts of lysates (50 μg) were incubated with 50 μM Ac-DEVD-MCA at 37 °C for 30 min to measure caspase-3-like activity using a spectrophotometer with excitation at 380 nm and emission at 460 nm. (b) Vulnerability of caspase-12-overexpressing cells compared with mock-expressing cells. After treatment with 1.0 μg/ml Tm for 20 h, culture medium was harvested for LDH assay by the manufacturer's protocol (KYOKUTO, Japan). Data are the mean of four independent experiments.

This study showed that activation of exogenous murine caspase-12 led to activation of cytoplasmic caspase-3, rather than caspase-9, in ER stress-induced apoptosis. We also showed by electron microscopy that ER stress inducers cause ER swelling prior to mitochondrial disruption. These findings suggested that cross-talk between these ER and cytoplasmic caspases is important for ER stress-induced apoptosis in SK-N-SH cells, rather than ER-mitochondrial cross-talk [4,15]. This possibility was recently supported by Rao et al. [11]. There have been several reports on the molecular mechanism of caspase-12 activation [9,12,18], so caspase-12 may play a role in apoptosis after ER stress.

Human caspase-12 has not been cloned yet and there is controversy about its expression [2,12]. Consequently, we investigated murine caspase-12 as a substitute for endogenous human caspase-12-like protease. Future isolation and functional analysis of human caspase-12 may lead to better understanding of ER stress-induced apoptosis in human cells.

References

[1] T. Fernandes-Alnemri, R.C. Armstrong, J. Krebs, S.M. Srinivasula, L. Wang, F. Bullrich, L.C. Fritz, J.A. Trapani, K.J. Tomaselli, G. Litwack, E.S. Alnemri, In vitro activation of CPP32 and Mch3 by Mch4, a novel human apoptotic cysteine protease containing two

FADD-like domains, Proc. Natl. Acad. Sci. USA 93 (1996) 7464–7469.

[2] H. Fischer, U. Koenig, L. Eckhart, E. Tschachler, Human caspase 12 has acquired deleterious mutations, Biochem. Biophys. Res. Commun. 293 (2002) 722–726.

[3] M.J. Gething, J. Sambrook, Transport and assembly processes in the endoplasmic reticulum, Semin. Cell Biol. 1 (1990) 65–72.

[4] O. Hori, F. Ichinoda, T. Tamatani, A. Yamaguchi, N. Sato, K. Ozawa, Y. Kitao, M. Miyazaki, M. Harding, D. Ron, M. Tohyama, D. Stern, S. Ogawa, Transmission of cell stress from endoplasmic reticulum to mitochondria: enhanced expression of Lon protease, J. Cell Biol. 157 (2002) 1151–1160.

[5] T. Katayama, K. Imaizumi, N. Sato, K. Miyoshi, T. Kudo, J. Hitomi, T. Morihara, T. Yoneda, F. Gomi, Y. Mori, Y. Nakano, J. Takeda, T. Tsuda, Y. Itoyama, O. Murayama, A. Takashima, P. St George-Hyslop, M. Takeda, M. Tohyama, Presenilin-1 mutations down-regulate the signalling pathway of the unfolded-protein response, Nat. Cell Biol. 1 (1999) 479–485.

[6] R.J. Kaufman, Stress signaling from the lumen of the endoplasmic reticulum: coordination of gene transcriptional and translational controls, Genes Dev. 12 (1999) 1221–1233.

[7] Y. Kozutsumi, M. Segal, K. Normington, M.J. Gething, J. Sambrook, The presence of malfolded proteins in the endoplasmic reticulum signals the induction of glucose-regulated proteins, Nature 332 (1988) 462–464.

[8] X. Liu, C.N. Kim, J. Yang, R. Jemmerson, X. Wang, Induction of apoptotic program in cell-free extracts: requirement for dATP and cytochrome c, Cell 86 (1996) 147–157.

[9] T. Nakagawa, J. Yuan, Cross-talk between two cysteine protease families. Activation of caspase-12 by calpain in apoptosis, J. Cell Biol. 150 (2000) 887–894.

[10] T. Nakagawa, H. Zhu, N. Morishima, E. Li, J. Xu, B. Yankner, J. Yuan, Caspase-12 mediates endoplasmic-reticulum-specific apoptosis and cytotoxicity by amyloid-beta, Nature 403 (2000) 98–103.

[11] R.V. Rao, S. Castro-Obregon, H. Frankowski, M. Schuler, V. Stoka, G. del Rio, D.E. Bredesen, H.M. Ellerby, Coupling endoplasmic reticulum stress to the cell death program. An Apaf-1-independent intrinsic pathway, J. Biol. Chem. 277 (2002) 21836–21842.

[12] R.V. Rao, E. Hermel, S. Castro-Obregon, D.G. Rio, H.M. Ellerby, M. Ellerby, D.E. Bredesen, Coupling endoplasmic reticulum stress to the cell death program. Mechanism of caspase activation, J. Biol. Chem. 276 (2001) 33869–33879.

[13] N. Sato, O. Hori, A. Yamaguchi, J.C. Lambert, M.C. Chartier-Harlin, P.A. Robinson, A. Delacourte, A.M. Schmidt, T. Furuyama, K. Imaizumi, M. Tohyama, T. Takagi, A novel presenilin-2 splice variant in human Alzheimer's disease brain tissue, J. Neurochem. 72 (1999) 2498–2505.

[14] N. Sato, K. Imaizumi, T. Manabe, M. Taniguchi, J. Hitomi, T. Katayama, T. Yoneda, T. Morihara, Y. Yasuda, T. Takagi, T. Kudo, Y. Itoyama, T. Makifuchi, P.E. Fraser, P. St George-Hyslop, M. Tohayama, Increased production of beta-amyloid and vulnerability to endoplasmic reticulum stress by an aberrant spliced form of presenilin 2, J. Biol. Chem. 276 (2000) 2108–2114.

[15] L. Scorrano, S.A. Oakes, J.T. Opferman, E.H. Cheng, M.D. Sorcinelli, T. Pozzan, S.J. Korsmeyer, BAX and BAK regulation of endoplasmic reticulum Ca^{2+}: a control point for apoptosis, Science 300 (2003) 135–139.

[16] N.A. Thornberry, Y. Lazebnik, Caspases: enemies within, Science 281 (1998) 1312–1316.

[17] A.A. Wehlinda, W. Tirasophon, R.J. Kaufman, The cellular response to protein misfolding in the endoplasmic reticulum, Gene Expr. 7 (1999) 293–300.

[18] T. Yoneda, K. Imaizumi, K. Oono, D. Yui, F. Gomi, T. Katayama, M. Tohyama, Activation of caspase-12, an endoplastic reticulum (ER) resident caspase, through tumor necrosis factor receptor-associated factor 2-dependent mechanism in response to the ER stress, J. Biol. Chem. 276 (2001) 13935–13940.

ELSEVIER

The cytosolic inclusion bodies that consist of splice variants that lack exon 5 of the presenilin-2 gene differ obviously from Hirano bodies observed in the brain from sporadic cases of Alzheimer's disease patients

Takayuki Manabe[a,b], Taiichi Katayama[a,b,*], Naoya Sato[a], Takashi Kudo[c], Shinsuke Matsuzaki[a,b], Kazunori Imaizumi[b,d], Masaya Tohyama[a,b]

[a]Department of Anatomy and Neuroscience, Graduate School of Medicine, Osaka University, 2-2 Yamadaoka, Suita, Osaka 565-0871, Japan
[b]CREST, Japan Science and Technology (JST), 2-2 Yamadaoka, Suita, Osaka 565-0871, Japan
[c]Department of Clinical Neuroscience, Psychiatry, Graduate School of Medicine, Osaka University, 2-2 Yamadaoka, Suita, Osaka 565-0871, Japan
[d]Division of Structural Cell Biology, Nara Institute of Science and Technology (NAIST), 8916-5 Takayama, Ikoma, Nara 630-0101, Japan

Abstract

Alzheimer's disease (AD) is a neurodegenerative disorder having several pathological characteristics, namely senile plaques and neurofibrillary tangles. Further, Hirano bodies (HBs), which are stained by hematoxylin-eosin, are also observed in the AD brain. Recently, we reported that an alternative splice variant that lacked exon 5 of the presenilin-2 (PS2) gene (PS2V) was expressed in sporadic AD (SAD) brains, and the PS2V-encoding proteins actually existed in these brains. Furthermore, electron microscopic experiments demonstrated that the PS2V proteins form cytosolic inclusion bodies in the pyramidal cells. In this report, we found that the PS2V-composed inclusion bodies differed obviously from the HBs. This observation suggests the possibility that PS2V-composed inclusions are a novel inclusion body, compared with other pathological characteristics previously reported in the SAD brain. We named this inclusion body the 'PS2V body'. © 2002 Elsevier Science Ireland Ltd. All rights reserved.

Recently, many aberrant splice forms of particular genes in some neurodegenerative disorders were reported, for example, the EAAT2 gene that is a glutamate transporter in amyotrophic lateral sclerosis [6], the tau gene that is involved in frontotemporal dementia and parkinsonizm (FTDP-17) [5], the presenilin-1 (PS1) gene that is involved in familial Alzheimer's disease [8,13] and so on. Furthermore, we have reported that the alternative splice form that lacked exon 5 of the presenilin-2 (PS2) gene (PS2V) also existed in the brain of the sporadic cases of Alzheimer's disease (SAD) patients [10]. PS2V encodes the N-terminal protein of PS2, which contain residues Met1-Leu119 and

five additional amino acid residues (SSMAG) at its C-terminus.

Alzheimer's disease (AD) is a neurodegenerative disorder, and over 90% of AD patients are SAD. The AD patients possess clinical characters that include progressive loss of memory and other cognitive abilities. Its pathological characteristics include neuronal losses, glial proliferations and accumulations of intraneuronal neurofibrillary tangles and extracellular depositions of senile plaques composed primarily of beta-amyloid (Aβ) [12]. In addition to these characteristics, we proposed the additional pathological characteristics of PS2V-encoded aberrant proteins in apoptotic pyramidal cells of the cerebral cortex and in the hippocampal CA1 region in 100% of SAD brains as assayed by immunohistochemical analysis [11]. Furthermore, these inclusion bodies do not co-localize with anti-Aβ antibody-positive senile plaques and anti-tau antibody-positive intra-

* Corresponding author. Tel.: +81-6-6879-3221; fax: +81-6-6879-3229.
E-mail address: katayama@anat2.med.osaka-u.ac.jp (T. Katayama).
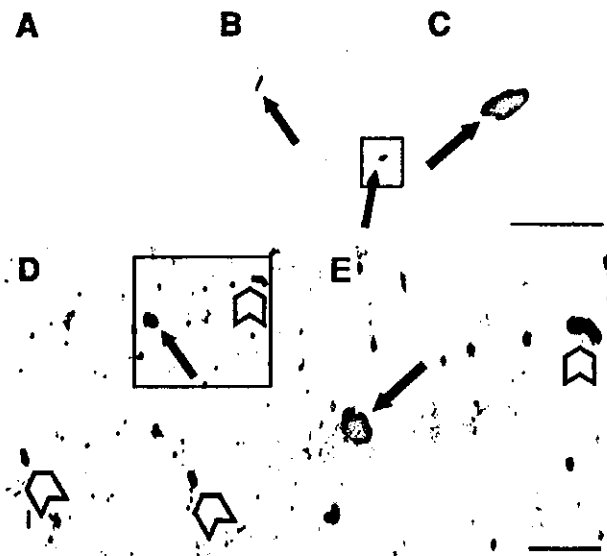
Fig. 1. Immunohistochemistry of PS2V-composed inclusions and HE-staining of HBs. (A–C) Controls (A); and SAD brains (B and C) cut at a thickness of 10 μm for subsequent immunohistochemical detection of PS2V-composed inclusions. (D–E) Sections from SAD brain were primary stained using an immunohistological method, as well as (A–C), followed by secondary counter-stained using HE. C and E are enlargements of B and D, respectively. Black and white arrows indicated PS2V-composed inclusion bodies and HE positive HBs, respectively. Scale bar, 4 μm.

Table 1
Comparison of the dimensions between PS2V-composed inclusions and HBs[a]

	Diameter (% of HBs)		Long/short
	Long axis	Short axis	
HBs (n = 17)	100 ± 31.7	100 ± 27.8	3.1
PS2V-composed inclusions (n = 8)	128.8 ± 39.7	192.8 ± 39.2	2.0

[a] The length of long and short axis of each inclusion were measured and shown as percentage of HBs (mean ± SE is shown). The ratios of long axis against short axis were shown (long/short).

neuronal neurofibrillary tangles [11]. However, it is unknown whether the PS2V-composed inclusion bodies co-localize with Hirano bodies (HBs) that are another pathological indicator associated with the AD brain.

The HBs are large-sized eosinophilic intracytoplasmic inclusions and are found in several neurodegenerative disorders, including AD [3,4,9]. Further, the HBs are observed in the hippocampal pyramidal cell layers of the AD brain [2]. HBs have been shown to express epitopes for various cytos-

keletal components like actin, actin binding protein, α-actin, vinculin, and low and medium molecular weight neurofilament protein [7].

According to these previous reports, PS2V-composed inclusion bodies and HBs indicate similar pathological conditions. Therefore, we compared the immunoreactive PS2V-composed inclusions with HBs in the hippocampal CA1 region in SAD brain tissue using an immunohistochemical approach.

More potent expression of immunoreactive splice variants that lacked exon 5 of the PS2 gene (PS2V) was observed in the hippocampal CA1 region of SAD brains (Figs. 1B,C), than in age-matched controls (Fig. 1A), which is consistent with a previous report [11]. Further, electron microscopic experiments demonstrated that these immunoreactive signals formed inclusion bodies in the cytoplasm of pyramidal cells from the hippocampus of cases of SAD (data not shown) [11]. The specificity of the antibodies against PS2V, which specifically recognize the C-terminal SSMAG residues of PS2V, were previously demonstrated and described [11]. Further, we have previously reported that PS2V-composed inclusions were close to anti-amyloid-beta (Aβ) antibody-positive senile
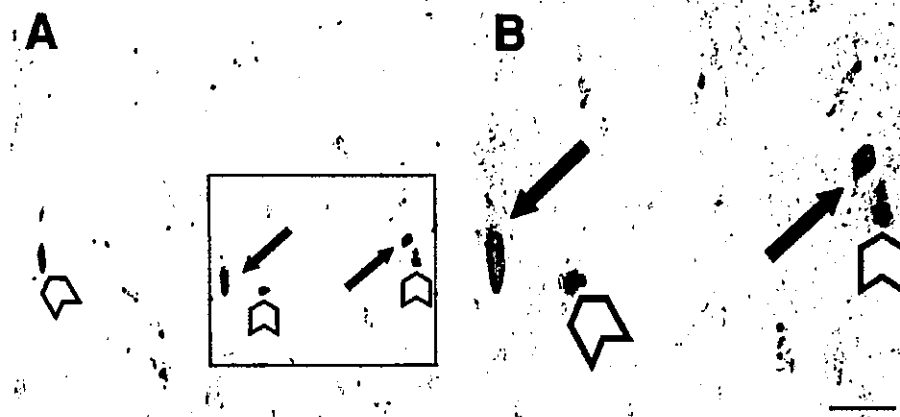

Fig. 2. Immunohistochemistry of PS2V-composed inclusions and HBs. (A, B) SAD brains were cut at a thickness of 10 μm for subsequent immunohistochemical detection of PS2V-composed inclusions and anti-α-actin antibody-positive HBs. B is an enlargement of A. Black and white arrows indicated PS2V-composed inclusion bodies and anti-α-actin antibody positive HBs, respectively. Scale bar, 4 μm.